Reviewer 1:

This study developed the unit-based industrial emission inventory in Beijing-Tianjin-Hebei region, for which configurations and locations of individual industrial emission sources were utilized. Significant differences in horizontal distributions of emissions were seen by comparing with the traditional proxy-based emission inventory. The air quality simulations using this unit-based emission inventory showed better model performance than the proxy-based emission inventory.

I think this is an important progress to get better model performance. It should contribute to developing effective emission controls against heavy air pollution in this region. However, various critical information is missing in the current manuscript. It is necessary to revise it based on the comments described below.

Response: We appreciate the reviewer's valuable comments which help us improve the quality of the manuscript. We have carefully revised the manuscript according to the reviewers' comments. Point-to-point responses are given below. The original comments are in black, while our responses are in blue.

(1) As mentioned in the introduction, previous studies have already developed unit-based emission inventories while their target sectors may be limited. I suppose there should be more papers including Liu et al. (2015) for example. It is necessary to clearly describe what is new in this study. This manuscript says previous studies did not cover all industrial sectors in the BTH region. Then, does this study cover all industrial sectors? Which sectors were newly included? Is the methodology identical for the sectors which have been already included in previous studies? Significance of this study should be described more clearly.

Response: We thank the reviewer for this valuable comment. We searched the papers about unit-based emission inventories again and added more papers in the Introduction section, including Liu et al. (2015) about emission from coal-fired power plants, Chen et al. (2015) about emission from cement industry and Wu et al. (2015) about emission from steel industry. (Page 3, Line 13-16) In the previous studies, they usually focus on one or several sectors such as power plant, cement plant, and iron plant. In this study, we cover most industrial sectors including power plant, industrial boiler, iron and steel production, non-ferrous metal smelter, coking, cement, glass, brick, lime, ceramics, refinery, and chemical industries (Page 4, Line 3-5). Compared with most previous studies, industrial boiler, non-ferrous metal smelter, coking, glass, brick, lime, ceramics, refinery, and chemical industries are newly included. The methodology of calculating the emission of point sources is similar to previous studies, but we calculate the emissions from cement and iron sectors according to specific industrial processes, such as clinker burning and clinker processing stages in the cement sector (Page 4, Line 18 to Page 5, Line 5).

(2) One of difficulties in unit-based emission inventories we often face is consistency of energy consumption against energy statistics. Did this study use energy consumption reported from each emission source? If so, is the sum of the reported energy consumption consistent with that in energy statistics? Usually, it is very hard to collect detailed information of small emission sources. If this is the case, energy consumption should not be consistent, and a hybrid approach in which unit-based and proxy-based information are combined may be necessary for each sector. The unit-based and proxy-based emission inventories were compared in this study. Do energy consumptions used in both inventories match?

Response: Yes, this study calculated emissions using energy consumption or industrial production reported for each emission source.

The plants in this study are from compilation of power industry statistics (China Electricity Council, 2015), China Iron and Steel Industry Association (http://www.chinaisa.org.cn), China Cement Association (http://www.chinacca.org), Chinese environmental statistics (collected from provincial environmental protection bureaus), the first national census of pollution sources (National Bureau of Statistics (NBS), 2010) and bulletin of desulfurization and denitrification facilities from Ministry of Ecology and Environment of China (http://www.mee.gov.cn). (Page 5, Line 6-13)

We compared the sum of the energy consumption or industrial production for each plant with those in official statistics. The sum of individual plants generally accounts for over 90% of the energy consumption or product yield reported in the statistics. For the plants not included in the preceding data sources, we calculate the emission by using "top-down method" and allocate the emission with proxies, such as GDP and population. Therefore, the total energy consumption of both inventories match. (Page 6, Line 14-17; Page 7, Line 25-26)

(3) Although detailed descriptions for vertical distributions are missing in the current manuscript, I agree that reasons of differences in concentrations between the unit-based and proxy-based emission inventories should be horizontal distributions and vertical distributions as mentioned in the second paragraph in the page 9. According to Figures 5 and 7, concentrations simulated with the proxy-based emissions are almost entirely lower throughout the domain. If influences of horizontal distributions are dominant, it is supposed that concentrations in surrounding regions would become higher, but such influences seem to be very limited. Therefore, it might be possible that differences in concentrations between two emission inventories are mainly caused by differences in vertical distributions of emissions. I would strongly recommend conducting an additional simulation to separate influences of horizontal and vertical distributions of emissions by changing only each of them.

Response: We thank the reviewer for this valuable comment. We have conducted an additional simulation in which the unit-based inventory is used but the emission heights are assumed to be the same as the proxy-based inventory. The amount of emission is the same as the other two scenarios. We call the inventory used in this simulation "hypo unit-based inventory".

Fig. R1 (Fig. 5 in the revised manuscript) shows the distribution of the monthly (January and July) mean concentrations of SO_2, NO_2, ozone, daily maximum 1-h averaged ozone, daily maximum 8-h averaged ozone and $PM_{2.5}$ simulated with the proxy-based inventory, and the differences between the proxy-based simulation and the other two simulations (Diff1: hypo unit-based minus proxy-based; Diff2: unit-based minus proxy-based). For SO_2, NO_2 and $PM_{2.5}$, the concentrations in the urban area are generally higher with the proxy-based inventory than those with the unit-based inventory, especially in winter. In January, large concentration differences between simulations with two inventories are found in urban Tianjin, Tangshan, Baoding and Shijiazhuang, where a large amount of industrial emissions is allocated in the proxy-based inventory due to large population density. The simulation of July follows the same pattern but the concentrations and the difference between the concentrations with two inventories are lower than those of January. In some areas where many factories are located, such as the northern part of Xingtai city, the concentration with unit-based inventory is higher because of a high emission intensity. There are two reasons for the difference between results with proxy-based and unit-based inventories. The first one is the spatial distribution. With detailed information of industrial sectors, more emissions are allocated to certain locations in suburban/rural areas in the unit-based emission inventory. From "Diff1" (hypo unit-based minus proxy-based), we can see that the improved horizontal distribution of the unit-based emission inventory significantly decreases the $PM_{2.5}$, SO_2, and NO_2 concentrations in most urban centers, and significantly increases the concentrations in a large fraction of suburban and rural areas, especially the areas where large industrial plants are located in. The other reason is vertical distribution. Plume rise is calculated in the simulation with the unit-based inventory, which causes the difference of emissions in vertical layers. The higher the pollutants are emitted, the lower the ground concentration becomes. From the differences between Diff1 and Diff2 we can see that the plume rise leads to lower concentrations over the whole region.

The results of the additional simulation have been added to the revised manuscript (Page 11, Line 6 to 26; Page 14, Line 2-4)

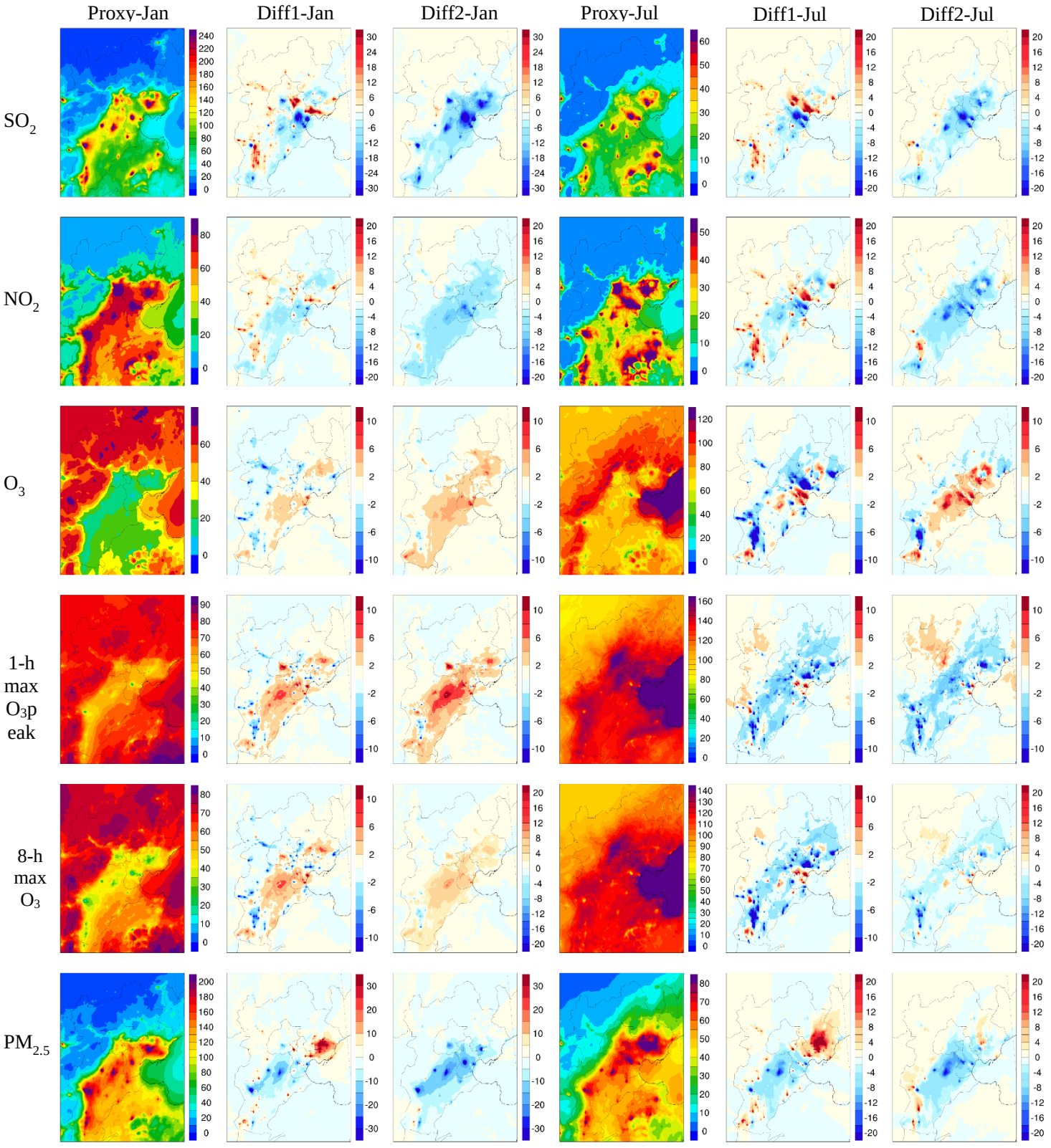

Fig. R1 Spatial distribution of the monthly (January and July) mean concentrations of SO_2, NO_2, ozone, daily maximum 1-h averaged ozone, daily maximum 8-h averaged ozone and $PM_{2.5}$ simulated with the proxy-based inventory, and the differences between the proxy-based simulation and the other two simulations (Diff1: hypo unit-based minus proxy-based; Diff2: unit-based minus proxy-based). The units are $\mu g/m^3$ for all panels.

(4) This paper shows relative improvements in the unit-based emission inventory by comparing with the proxy-based emission inventory. Therefore, relative changes depend not only on the unit-based inventory but also the proxy-based inventory. If poor proxies are used in the proxy-based inventory, relative improvements could become larger. Therefore, it is important to explicitly show which proxies were used in the proxy-based inventory for each sector (not just "such as population …" at the end of the section 2.2). Use of better proxies should be also one of possible directions to get better model performance.

Response: For the proxies of each sector, we refer to Zhao et al. (2013), Streets et al. (2003) and Woo et al. (2003). We allocate the emissions of each province and each pollutant by two steps. The first step is to allocate the total emission to each county. The second step is to allocate the emission of each county to each grid. The proxies used in this study are shown in Table R1 (Table S2 in the revised manuscript).

Table R1 Proxies used in the proxy-based inventory for each sector

Sector	Allocate to county	Allocate to grid
Power plant, steel, cement	GDP of secondary industry	Population density
Industrial combustion, other industrial process	GDP of secondary industry	Population density
Domestic fuel	Total GDP	Population density
Domestic biomass	GDP of first industry	Population density
Transportation	GDP of tertiary industry	Road network
Open burning	GDP of first industry	Population density
Livestock	GDP of first industry	Population density
Fertilizer application	GDP of first industry	Population density
Domestic solvent use	Total GDP	Population density
Industrial solvent use	GDP of secondary industry	Population density

(5) Page 3, Line 9-10

I think that Lim et al. (2005) is not related to the description around here.

Response: It is removed from the manuscript.

(6) Page 3, Line 17-18

It is not clear which sectors are considered in previous studies and which sectors newly appear in this study. I would recommend adding a table listing all the industrial sectors considered and which are new in this study.

Response: As is shown in Table R2. The underlined sectors are newly added to this study. This table is added to SI. (Table S3)

Table R2 Comparison of industrial sectors covered in previous studies and this study (the underlined sectors are newly included in this study).

Study	Sector	Region
Zhao et al. (2008), Chen et al. (2014), Liu et al. (2015), Li et al. (2017)	Power plants	China
Wang et al. (2016b), Wu et al. (2015)	Iron plants	China

Lei et al. (2011), Chen et al. (2015)	Cement plants	China
Qi et al. (2017)	Power plants, iron plants, cement factories, coking factories, heating plants, other industries	BTH
This study	Power plants, iron plants, cement factories, coking factories, nonferrous metals, glass factories, brick factories, lime factories, ceramics factories, refinery factories, chemical plants, industrial boilers	BTH

(7) Page 4, Line 6-7

It is not clear what kind of product yields are used for estimating emissions of each sector. I would recommend showing types of products used for each sector in a table I recommended above.

Response: The types of products used for each sector are listed as follows and in Table S4 of the revised manuscript.

Table R3 Types of products or energy consumption used for estimating emissions of each sector.

Industrial sector	**Product or energy consumption**
Power plant	Energy consumption
Industrial boiler	Energy consumption
Iron and steel production	Pig iron, crude steel, rolled steel
Non-ferrous metal smelter	Alumina, aluminum, copper
Coking	Coke
Cement	Cement, clinker
Glass	Glass
Brick	Brick
Lime	Lime
Ceramics	Ceramics
Refinery	Crude oil, ethylene
Chemical industries	Ammonia, caustic soda, soda ash, sulfuric acid, nitric acid

(8) Page 4, Lines 9 and 17

The equation (1) is used to estimate emissions of the pollutant i. The industrial enterprise j and the production process m appear in this equation, but they are summed up. Then, how about the control technology n? It is not summed up, but it does not

appear in the left-hand side. Usually fractions of control technologies are inserted, then they are summed up for all of control technologies. This is the same for the control technology k in the equation (2).

Response: Equation (1) and equation (2) are revised as follows:

$$E_{i,j} = A_j \times EF_{i,j} \times \left(1 - \eta_{i,j}\right) \qquad (1)$$

where $E_{i,j}$ is emissions of pollutant i from industrial enterprise j, A_j is activity level of industrial enterprise j, $EF_{i,j}$ is uncontrolled emission factor of pollutant i from industrial enterprise j, and $\eta_{i,j}$ is removal efficiency of pollutant i by control technology in enterprise j. $\eta_{i,j}$ is determined by the production process and control technology of the industrial enterprise. The $EF_{i,j}$, which depends on the production process of the industrial enterprise, are calculated according to the sulfur and ash contents of fuels (e.g. coal) used in each province (for PM and SO_2), or obtained from our previous study (Zhao et al., 2013) (for other pollutants).

For those industrial sources with multiple production processes, such as iron and steel production and cement production, emissions are calculated by using the following equation:

$$E_{i,j} = \sum_m \left(AK_{j,m} \times EF_{i,m} \times \left(1 - \eta_{i,j,m}\right)\right) + \left(AC_j \times ef_i \times \left(1 - \eta_{i,j}\right)\right) \qquad (2)$$

where $E_{i,j}$ is emissions of pollutant i from industrial enterprise j, $AK_{j,m}$ is the amount of clinker produced by the clinker burning process m of the enterprise j, $EF_{i,m}$ is uncontrolled emission factor for pollutant i from the clinker burning process m, $\eta_{i,j,m}$ is removal efficiency of pollutant i from the clinker burning process m in enterprise j, AC_j is the amount of cement produced by enterprise j, ef_i is uncontrolled emission factors from the clinker processing stage (ef_i=0 if i is not particulate matter), $\eta_{i,j}$ is removal efficiency of pollutant i in enterprise j. $\eta_{i,j,m}$ and $\eta_{i,j}$ both depend on the control technology of the industrial enterprise. (Page 4, Line 10 to Page 5, Line 2)

(9) Page 4, Lines 9 and 17

I do not understand why the equations (1) and (2) are separated. It seems the first and second terms of the equation (2) represent clinker and cement production, respectively. However, isn't it possible to treat both as one of production processes m? If not, then what are production processes considered in both equations? Please clarify them. In fact, it is not clear what production processes considered in this study are.

Response: Equations (1) and (2) cannot be merged because the production processes represented by the first and second terms of equation (2) are frequently performed in different enterprises. For example, for cement production, clinker may be produced in one enterprise and subsequently processed in another enterprise, which is very common.

Most industrial sources are calculated by equation (1). Only a few industrial sources with multiple processes, such as steel production and cement production, are calculated by equation (2). We have added the preceding descriptions in the revised manuscript (Page 4, Line 18-19; Page 5, Line 3-5).

(10) Page 4, Lines 12-14

EFs depend only on the pollutant i and the production process m. Is there any possibility to use emission factors specific to each industrial enterprise? Is it enough to use identical emission factors for all the industrial enterprises?

Response: For SO_2 and PM, EFs are calculated according to the sulfur and ash contents of fuels (e.g. coal) in each province. For other pollutants, EFs depend only on the pollutant and the production process, and are obtained from our previous studies (Zhao et al., 2013). (Page 4, Line 14-17)

We agree with the reviewer that it is better to use emission factors specific to each individual enterprise. However, such detail offline emission measurements are not yet available in China. The continuous emission monitoring systems (CEMS) data may help to improve the emission esitmates. Cui et al. (2018) estimated the emissions of air pollutants from power plants in China based on the data of CEMS, environmental statistics and the data of pollutant emission permits. (Karplus et al., 2018) evaluated the impact of China's new air pollution standards on SO_2 emissions by comparing newly available data from CEMS with satellite measurements. We will work on it in the future.

(11) Page 4, Line 25 – Page 5, Line 1

Specific references are not listed here while a lot of specific references for proxy-based emissions are listed in a subsequent paragraph. Specific references should be also listed for unit-based emissions as much as possible.

Response: The references were added in this manuscript.

For all power and industrial sources except industrial boilers, we collect their detailed information, including latitude/longitude, annual product, production technology/process, and pollution control facilities from compilation of power industry statistics (China Electricity Council, 2015), China Iron and Steel Industry Association (http://www.chinaisa.org.cn), China Cement Association (http://www.chinacca.org), Chinese environmental statistics (collected from provincial environmental protection bureaus), the first national census of pollution sources (National Bureau of Statistics (NBS), 2010) and bulletin of desulfurization and denitrification facilities from Ministry of Ecology and Environment of China (http://www.mee.gov.cn). (Page 5, Line 6-13)

(12) Page 5, Lines 2-4

Do these numbers cover all the plants located in the target area?

Response: It's very difficult to cover all the plants located in Beijing-Tianjin-Hebei region because there are some very small factories. The plants in this study are from compilation of power industry statistics (China Electricity Council, 2015), China Iron and Steel Industry Association (http://www.chinaisa.org.cn), China Cement Association (http://www.chinacca.org), Chinese environmental statistics (collected

from provincial environmental protection bureaus), the first national census of pollution sources (National Bureau of Statistics (NBS), 2010) and bulletin of desulfurization and denitrification facilities from Ministry of Ecology and Environment of China (http://www.mee.gov.cn). The sum of individual plants generally accounts for over 90% of the energy consumption or product yield reported in the statistics. For the plants not included in the preceding data sources, we calculate the emission by using "top-down method" and allocate the emission with proxies, such as GDP and population. (Page 5, Line 6-13; Page 6, Line 14-18; Page 7, Line 25-26)

(13) Page 5, Line 5

Is there no information on control technologies for boilers?

Response: We do have information on control technologies for boilers. This sentence was revised as: "For industrial boilers, we obtained the location, fuel use amount, and control technologies of over 8 thousand industrial boilers…" (Page 5, line 16-19)

(14) Page 5, Line 9

Is the expression "emission factor method" appropriate? The unit-based approach also uses emission factors. I think it is usually called as "top-down method" (but sometimes confused with top-down estimates utilizing observations including satellites).

Response: "emission factor method" was replaced with "top-down method" in this sentence. (Page 6, Line 7)

(15) Page 5, Line 17

How about speciation of PM2.5 and NMVOCs for unit-based emissions?

Response: As is described in the manuscript, the speciation of $PM_{2.5}$ is from Fu et al. (2013). The $PM_{2.5}$ speciation profile of major sectors is shown in Fig. R2 (Fig. S4 in the manuscript). The speciation of NMVOCs is updated by Wu et al. (2017). The speciation profiles used in the unit-based inventory is the same as those used in the proxy-based inventory. The manuscript is revised accordingly. (Page 6, Line 18-20)

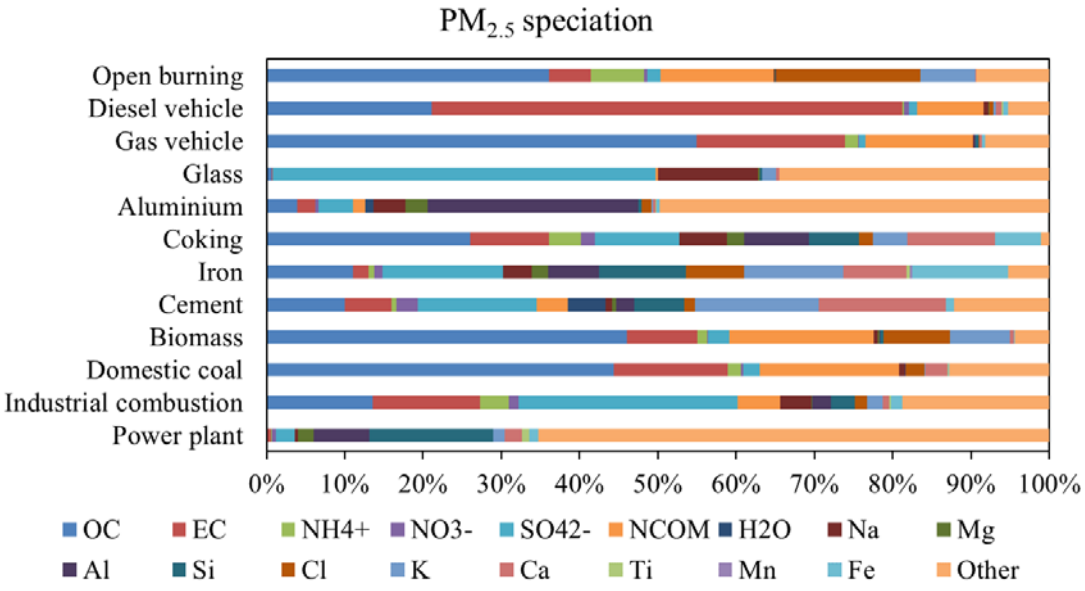

Fig. R2 $PM_{2.5}$ speciation profile of major sectors

(16) Page 5, Line 20 – Page 6, Line 18
References for models and modules are required.
Response: References are added to the manuscript. The revised text is shown as follows: In this work, we use CMAQ version 5.0.2 (EPA, 2014) to simulate the concentration of pollutants. (Page 6, Line 23-24) The Carbon Bond 05 (CB05) and AERO6 (Sarwar et al., 2011) are chosen as the gas-phase and aerosol chemical mechanisms, respectively. (Page 7, Line 5-7)
We use the Weather Research and Forecasting (WRF) model version 3.7.1 (Skamarock et al., 2008) to simulate the meteorological fields. The physics options for the WRF simulation are the Kain-Fritsch cumulus scheme (Kain, 2004), the Morrison double-moment scheme for cloud microphysics (Morrison et al., 2005), the Pleim-Xiu land surface model (Xiu and Pleim, 2001), Pleim-Xiu surface layer scheme (Pleim, 2006), ACM2 (Pleim) boundary layer parameterization (Pleim, 2007), and Rapid Radiative Transfer Model for GCMs radiation scheme (Mlawer et al., 1997). (Page 7, Line 9-14)

(17) Page 6, Line 10
What are “other” configurations? Please show explicitly.
Response: “Other” configurations means the initial and boundary conditions. The meteorological initial and boundary conditions are generated from the Final Operational Global Analysis data (ds083.2) of the National Center for Environmental Prediction (NCEP) at a $1.0^{o} \times 1.0^{o}$ and 6-h resolutions. Default profile data is used for chemical initial and boundary conditions. It is revised accordingly in the manuscript. (Page 7, Line 14-17)

(18) Page 6, Lines 21-23
Is CO not included in this study? Why?
Response: The ambient CO pollution is not a serious issue in China currently. According to China National Environmental Monitoring Centre (data source: http://106.37.208.233:20035/), the daily CO concentration in the BTH region is less than 1.5 mg/m^3, which is much lower than the national ambient air quality standard (4 mg/m^3). In addition, the influence of CO emission on the formation of $PM_{2.5}$ and O_3 is quite small. For these two reasons, we did not include CO emission in this study.
In the model simulations described in this paper, we used CO emissions developed by Janssens-Maenhout et al. (2015).

(19) Page 7 Lines 1-22
Area names are mentioned in these paragraphs. However, horizontal distributions firstly appear later in Fig. 3. Its description should appear before descriptions of areas.
Response: The sequence of these sentences has been adjusted. (Page 8, Line 12-13)

(20) Page 7, Line 6

It is impossible to see many industrial boilers in Fig. 2.

Response: The link was wrong and we revised it to “Fig. 3”. (Page 8, Line 12-13)

(21) Page 8, Line 9

I think that NMB and NME are not appropriate metrics in terms of this study. The target of this study is accurate horizontal distributions. However, overestimation in one areas and underestimation in other areas could be cancelled out in these metrics. It is necessary to appropriate metrics which can properly shows improvements realized in this study.

Response: Thank you for this valuable comment.

While the overestimation and underestimation in different areas could be cancelled out in normalized mean bias (NMB), they cannot be cancelled out in the normalized mean error (NME), which characterizes the absolute difference between observation and simulation. Similarly, mean fractional error (MFE) is also an index that will not cancel out the overestimation and underestimation. The NME and MFE for SO_2, NO_2, $PM_{2.5}$, and O_3 are mostly lower with the unit-based inventory than with the proxy-based inventory, which means that the spatial distributions of these pollutants are better captured using the unit-based inventory. (Page 12, Line 5-8)

A major difference between the proxy-based and unit-based inventories is that the traditional proxy-based inventory allocates more emission to the urban area, whereas the unit-based inventory allocates more emission to suburban area where more factories are located. To quantify the impact of changed emission distribution between urban and suburban areas, we introduced the metric of “concentration gradient”, which is defined as the ratios of urban concentrations to suburban concentrations. The concentration gradients simulated with the unit-based inventory agree much better with observations than those simulated with the proxy-based inventory, implying that the unit-based emission inventory better reproduces the distributions of pollutant emissions between the urban and suburban areas. (Page 12, Line 5-22)

In addition, most of the observational sites (70 out of 80) are located in urban area. (Page 9, Line 19-20) Therefore, the calculated NMB is dominated by the behavior of the urban sites, and is not likely to be significantly cancelled out by the limited suburban sites.

Finally, we have shown the model performance for major air pollutants at each individual site in Beijing in the revised Supplementary Information (Table S6-S9). For the urban sites, the concentrations of $PM_{2.5}$, SO_2 and NO_2 are much lower with the unit-based inventory than with the proxy-based inventory. For the suburban sites, however, the concentrations are either slightly higher or slightly lower with the unit-based inventory than with the proxy-based inventory. The situation for ozone is quite the opposite. The ozone concentration at urban sites is higher with the unit-based inventory than with the proxy-based inventory. In suburban sites, it is lower with the unit-based inventory than with the proxy-based inventory. In addition, for the simulations with the unit-based inventory, the NME and MFE of individual sites are usually lower than those with the proxy-based inventory while the correlation efficient is usually higher, which means that the error is generally smaller and the trend is more

similar to the observation when the unit-based inventory is used.

(22) Page 8, Lines 15-17

What is a possible reason for the poor model performance on SO2?

Response: The overestimation of SO_2 concentrations may be due to the lack of several SO_2 reaction mechanisms in CMAQ, such as heterogeneous reactions of SO_2 on the surface of dust particles (Fu et al., 2016), the oxidation of SO_2 by NOx in aerosol liquid water (Cheng et al., 2016;Wang et al., 2016a), the effects of SO_2 and NH_3 on secondary organic aerosol formation (Chu et al., 2016), etc.

The biased spatial distribution of SO_2 emissions from residential combustion may also contribute to the overestimation. A large fraction of residential combustion takes place in the rural areas. In this work, however, the emission of residential combustion is allocated by GDP and population, which leads to an overestimation of SO_2 emission in urban area and hence an overestimation of SO_2 concentration. (Page 10, Line 4-11)

(23) Page 9, Lines 19-20

I cannot find any descriptions on plume rise before here. How to gather stack information? How to calculate plume rise? These descriptions are required in the method section.

Response: The stack information required for plume rise calculation includes stack height, flue gas temperature, chimney diameter and flue gas velocity. For power plants, we get the stack height from Compilation of power industry statistics (China Electricity Council, 2015). For the stack height of cement factories, we refer to the emission standard of air pollutants for cement industry (Ministry of Environmental Protection of China, 2013). For the stack height of glass, brick, lime and ceramics industries, we refer to emission standard of air pollutants for industrial kiln and furnace (Ministry of Environmental Protection of China, 1997). For the stack height of non-ferrous metal smelter, coking, refinery and chemical industries, as well as the flue gas temperature, chimney diameter and flue gas velocity for all industrial sectors, we refer to the national information platform of pollutant discharge permit (http://114.251.10.126/permitExt/outside/default.jsp), where we can find very detailed information of the plants with the pollutant discharge permit. For the sources without the pollutant discharge permit, we use the parameters of the plant with a similar production output or coal consumption. (Page 5, Line 23 to Page 6, Line 5) The data source of stack information is shown in Table R4 (Table S5 in the manuscript).

Table R4 Data source of stack information

Sector	Stack height	Flue gas temperature, Chimney diameter, Flue gas velocity
Power plant	Compilation of power industry statistics	National information platform of pollutant discharge permit
Cement plant	Emission standard of air pollutants for cement industry	

Glass, brick, lime and ceramics industries	Emission standard of air pollutants for industrial kiln and furnace
Non-ferrous metal smelter, coking, refinery and chemical industries	National information platform of pollutant discharge permit

Plume rise is calculated with a built-in algorithm of CMAQ based on the Briggs's scheme (Briggs, 1982). In this algorithm, plume rise is estimated by simulating the buoyancy effect and momentum rise, using hourly and gridded meteorological data. Then, the plume is distributed into the vertical layers that the plume intersects based on the pressure in each layer. (Page 5, Line 20-22; Page 8, Line 3-5)

(24) Page 10, Line 1

Details of "concentration gradient" are necessary. How to select urban and suburban locations? Are monthly mean concentrations used?

Response: For Beijing, the suburban areas refer to the districts that are far from the center of the city (the red star in Fig. 2). From Fig. 2 we can see that there are 8 sites located in the urban districts in Beijing. In the north, there are four sites far away from the city center and close to the city border. We treat the four sites in the north as suburban sites and the others as urban sites. For Tianjin, as shown in Fig. 3, there are two city centers. Ten sites are located in urban area and 5 sites are located in suburban area. In the calculation of the concentration gradient, monthly mean concentrations are used (Page 12, Line 10). These figures are added to the Supplementary Information. (Fig. S4-S5)

Fig. R3 The observational sites in Beijing

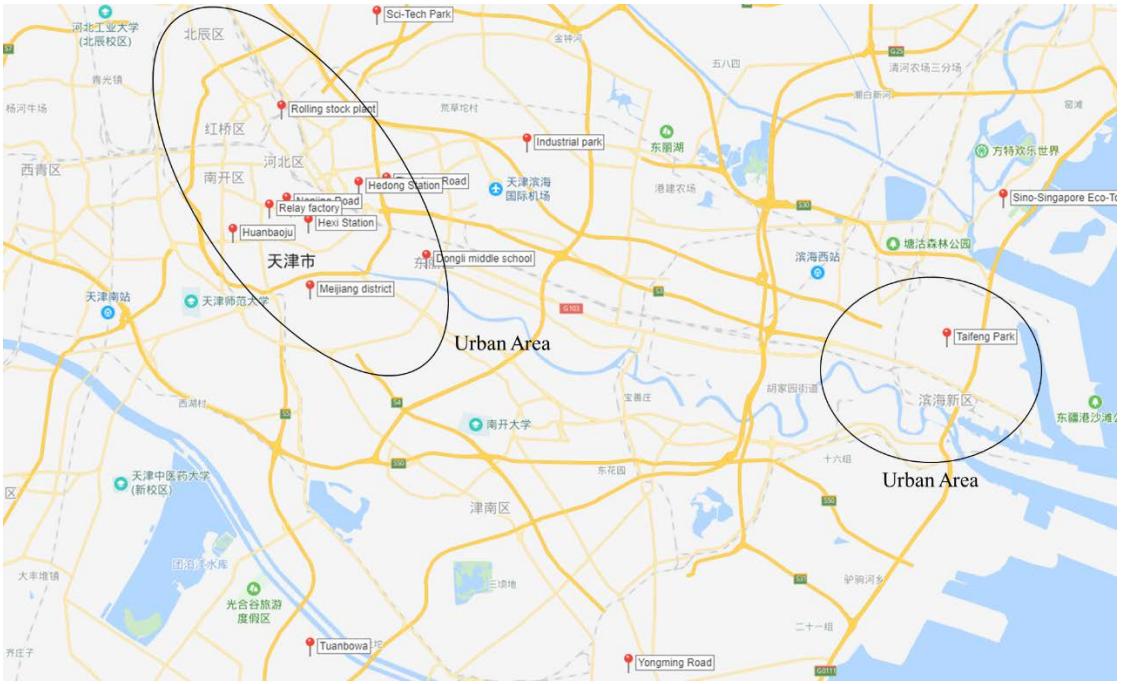

Fig. R4 The observational sites in Tianjin

(25) Page 10, Lines 24-27

I think it is not enough to explain changes of NO3- only by NOx sensitivities. I do not think they are main reasons. SO42- concentrations in the unit-based approach are much lower than the proxy-based approach whereas NH4+ is almost constant as shown in Fig.

7. In this case, more HNO3 is converted to NO3- with excess NH4+ whereas these processes depend on abundance of HNO3 or NH3.

Response: Thank you for the valuable idea. We have added this reason to explain the changes of NO_3^- as follows:

As for nitrate, concentration of nitrate in the simulation with unit-based inventory is much higher than that with proxy-based inventory in winter while the differences between the results with two inventories vary with location in summer. Sulfate concentrations in the unit-based approach are much lower than the proxy-based approach. In this case, more abundant NH_3 is available to react with HNO_3, leading to enhanced formation of NO_3^-. (Page 13, Line 11-14)

References:

Briggs, G. A.: Plume Rise Predictions, in: Lectures on Air Pollution and Environmental Impact Analyses, edited by: Haugen, D. A., American Meteorological Society, Boston, MA, 59-111, 1982.

Chen, L., Sun, Y., Wu, X., Zhang, Y., Zheng, C., Gao, X., and Cen, K.: Unit-based emission inventory and uncertainty assessment of coal-fired power plants, Atmos Environ, 99, 527-535, 10.1016/j.atmosenv.2014.10.023, 2014.

Chen, W., Hong, J., and Xu, C.: Pollutants generated by cement production in China, their impacts, and the potential for environmental improvement, Journal of Cleaner Production, 103, 61-69, 10.1016/j.jclepro.2014.04.048, 2015.

Cheng, Y., Zheng, G., Wei, C., Mu, Q., Zheng, B., Wang, Z., Gao, M., Zhang, Q., He, K., Carmichael, G., Poschl, U., and Su, H.: Reactive nitrogen chemistry in aerosol water as a source of sulfate during haze events in China, Science Advances, 2, 10.1126/sciadv.1601530, 2016.

China Electricity Council: Compilation of power industry statistics 2014, China Electricity Council, Beijing, 2015.

Chu, B., Zhang, X., Liu, Y., He, H., Sun, Y., Jiang, J., Li, J., and Hao, J.: Synergetic formation of secondary inorganic and organic aerosol: effect of SO₂ and NH₃ on particle formation and growth, Atmos Chem Phys, 16, 14219-14230, 10.5194/acp-16-14219-2016, 2016.

Cui, J., Qu, J., Bo, X., Chang, X., Feng, X., Mo, H., Li, S., Zhao, Y., Zhu, F., and Ren, Z.: High resolution power emission inventory for China based on CEMS in 2015, China Environmental Science, 38, 2062~2074, 2018.

CMAQv5.0.2 (Version 5.0.2), 2014.

Fu, X., Wang, S. X., Zhao, B., Xing, J., Cheng, Z., Liu, H., and Hao, J. M.: Emission inventory of primary pollutants and chemical speciation in 2010 for the Yangtze River Delta region, China, Atmos Environ, 70, 39-50, 10.1016/j.atmosenv.2012.12.034, 2013.

Fu, X., Wang, S., Chang, X., Cai, S., Xing, J., and Hao, J.: Modeling analysis of secondary inorganic aerosols over China: pollution characteristics, and meteorological and dust impacts, Sci Rep, 6, 35992, 10.1038/srep35992, 2016.

Janssens-Maenhout, G., Crippa, M., Guizzardi, D., Dentener, F., Muntean, M., Pouliot, G., Keating, T., Zhang, Q., Kurokawa, J., Wankmüller, R., Denier van der Gon, H., Kuenen, J. J. P., Klimont, Z., Frost, G., Darras, S., Koffi, B., and Li, M.: HTAP_v2.2: a

mosaic of regional and global emission grid maps for 2008 and 2010 to study hemispheric transport of air pollution, Atmos Chem Phys, 15, 11411-11432, 10.5194/acp-15-11411-2015, 2015.
Kain, J. S.: The Kain-Fritsch convective parameterization: An update, Journal of Applied Meteorology, 43, 170-181, 10.1175/1520-0450(2004)043<0170:tkcpau>2.0.co;2, 2004.
Karplus, V. J., Zhang, S., and Almond, D.: Quantifying coal power plant responses to tighter SO2 emissions standards in China, Proc Natl Acad Sci U S A, 115, 7004-7009, 10.1073/pnas.1800605115, 2018.
Lei, Y., Zhang, Q., Nielsen, C., and He, K.: An inventory of primary air pollutants and CO2 emissions from cement production in China, 1990-2020, Atmos Environ, 45, 147-154, 10.1016/j.atmosenv.2010.09.034, 2011.
Li, M., Zhang, Q., Kurokawa, J., Woo, J. H., He, K. B., Lu, Z. F., Ohara, T., Song, Y., Streets, D. G., Carmichael, G. R., Cheng, Y. F., Hong, C. P., Huo, H., Jiang, X. J., Kang, S. C., Liu, F., Su, H., and Zheng, B.: MIX: a mosaic Asian anthropogenic emission inventory under the international collaboration framework of the MICS-Asia and HTAP, Atmos Chem Phys, 17, 935-963, 10.5194/acp-17-935-2017, 2017.
Liu, F., Zhang, Q., Tong, D., Zheng, B., Li, M., Huo, H., and He, K. B.: High-resolution inventory of technologies, activities, and emissions of coal-fired power plants in China from 1990 to 2010, Atmos Chem Phys, 15, 13299-13317, 2015.
Ministry of Environmental Protection of China: Emission standard of air pollutants for industrial kiln and furnace, Ministry of Environmental Protection of China (MEP), Beijing, 1997.
Ministry of Environmental Protection of China: Emission standard of air pollutants for cement industry, Ministry of Environmental Protection of China (MEP), Beijing, 2013.
Mlawer, E. J., Taubman, S. J., Brown, P. D., Iacono, M. J., and Clough, S. A.: Radiative transfer for inhomogeneous atmospheres: RRTM, a validated correlated-k model for the longwave, J Geophys Res-Atmos, 102, 16663-16682, 10.1029/97jd00237, 1997.
Morrison, H., Curry, J. A., and Khvorostyanov, V. I.: A new double-moment microphysics parameterization for application in cloud and climate models. Part I: Description, Journal of the Atmospheric Sciences, 62, 1665-1677, 10.1175/jas3446.1, 2005.
National Bureau of Statistics (NBS): Report of the first national census of pollution sources, China Statistics Press, Beijing, 2010.
Pleim, J. E.: A simple, efficient solution of flux-profile relationships in the atmospheric surface layer, Journal of Applied Meteorology and Climatology, 45, 341-347, 10.1175/jam2339.1, 2006.
Pleim, J. E.: A Combined Local and Nonlocal Closure Model for the Atmospheric Boundary Layer. Part II: Application and Evaluation in a Mesoscale Meteorological Model, Journal of Applied Meteorology and Climatology, 46, 1396-1409, 10.1175/jam2534.1, 2007.
Qi, J., Zheng, B., Li, M., Yu, F., Chen, C., Liu, F., Zhou, X., Yuan, J., Zhang, Q., and He, K.: A high-resolution air pollutants emission inventory in 2013 for the Beijing-Tianjin-Hebei region, China, Atmos Environ, 170, 156-168,

10.1016/j.atmosenv.2017.09.039, 2017.
Sarwar, G., Appel, K. W., Carlton, A. G., Mathur, R., Schere, K., Zhang, R., and Majeed, M. A.: Impact of a new condensed toluene mechanism on air quality model predictions in the US, Geoscientific Model Development, 4, 183-193, 10.5194/gmd-4-183-2011, 2011.
Skamarock, W. C., Dudhia, J. B. K. J., Gill, D. O., Barker, D., Wang, W., and Powers, J. G.: A Description of the Advanced Research WRF Version 3, NCAR Technical Note NCAR/TN-475+STR, 10.5065/D68S4MVH, 2008.
Streets, D. G., Bond, T. C., Carmichael, G. R., Fernandes, S. D., Fu, Q., He, D., Klimont, Z., Nelson, S. M., Tsai, N. Y., Wang, M. Q., Woo, J. H., and Yarber, K. F.: An inventory of gaseous and primary aerosol emissions in Asia in the year 2000, Journal of Geophysical Research: Atmospheres, 108, 10.1029/2002jd003093, 2003.
Wang, G., Zhang, R., Gomez, M. E., Yang, L., Levy Zamora, M., Hu, M., Lin, Y., Peng, J., Guo, S., Meng, J., Li, J., Cheng, C., Hu, T., Ren, Y., Wang, Y., Gao, J., Cao, J., An, Z., Zhou, W., Li, G., Wang, J., Tian, P., Marrero-Ortiz, W., Secrest, J., Du, Z., Zheng, J., Shang, D., Zeng, L., Shao, M., Wang, W., Huang, Y., Wang, Y., Zhu, Y., Li, Y., Hu, J., Pan, B., Cai, L., Cheng, Y., Ji, Y., Zhang, F., Rosenfeld, D., Liss, P. S., Duce, R. A., Kolb, C. E., and Molina, M. J.: Persistent sulfate formation from London Fog to Chinese haze, Proc Natl Acad Sci U S A, 10.1073/pnas.1616540113, 2016a.
Wang, K., Tian, H., Hua, S., Zhu, C., Gao, J., Xue, Y., Hao, J., Wang, Y., and Zhou, J.: A comprehensive emission inventory of multiple air pollutants from iron and steel industry in China: Temporal trends and spatial variation characteristics, Sci Total Environ, 559, 7-14, 10.1016/j.scitotenv.2016.03.125, 2016b.
Woo, J. H., Baek, J. M., Kim, J. W., Carmichael, G. R., Thongboonchoo, N., Kim, S. T., and An, J. H.: Development of a multi-resolution emission inventory and its impact on sulfur distribution for Northeast Asia, Water Air and Soil Pollution, 148, 259-278, 10.1023/a:1025493321901, 2003.
Wu, W., Zhao, B., Wang, S., and Hao, J.: Ozone and secondary organic aerosol formation potential from anthropogenic volatile organic compounds emissions in China, J Environ Sci (China), 53, 224-237, 10.1016/j.jes.2016.03.025, 2017.
Wu, X., Zhao, L., Zhang, Y., Zheng, C., Gao, X., and Cen, K.: Primary Air Pollutant Emissions and Future Prediction of Iron and Steel Industry in China, Aerosol and Air Quality Research, 15, 1422-1432, 10.4209/aaqr.2015.01.0029, 2015.
Xiu, A. J., and Pleim, J. E.: Development of a land surface model. Part I: Application in a mesoscale meteorological model, Journal of Applied Meteorology, 40, 192-209, 10.1175/1520-0450(2001)040<0192:doalsm>2.0.co;2, 2001.
Zhao, B., Wang, S. X., Wang, J. D., Fu, J. S., Liu, T. H., Xu, J. Y., Fu, X., and Hao, J. M.: Impact of national NOx and SO2 control policies on particulate matter pollution in China, Atmos Environ, 77, 453-463, 10.1016/j.atmosenv.2013.05.012, 2013.
Zhao, Y., Wang, S. X., Duan, L., Lei, Y., Cao, P. F., and Hao, J. M.: Primary air pollutant emissions of coal-fired power plants in China: Current status and future prediction, Atmos Environ, 42, 8442-8452, 10.1016/j.atmosenv.2008.08.021, 2008.

Reviewer 2:

This is a timely paper that describes the development of a unit-based industrial emission inventory in northern China, which still suffers severe air pollution even though the government has put tremendous amount of effort in emission controls. A detailed, united-based emission inventory will be of great value when air quality models are used in developing/assessing emission control strategies. The paper is generally well-written. I would recommend the paper be published in ACP after addressing my comments below.

Response: We appreciate the reviewer's valuable comments which help us improve the quality of the manuscript. We have carefully revised the manuscript according to the reviewers' comments. Point-to-point responses are given below. The original comments are in black, while our responses are in blue.

(1) The paper lacks details on how vertical distribution of point source emissions are treated in the simulation. In the results section, it is mentioned that plume rise contributes to the difference between the CMAQ results. However, no details were provided on how the parameters needed for plume rise calculations are obtained. In my understanding, such data are not universally available (even in the US) so presumably the same situation is applicable in China. What is the criteria for selecting point sources for plume rise calculation and how missing information is estimated. I also believe that the authors should perform off-line emission vertical distribution calculations and compare with the empirical vertical distribution used for the proxy-based emission inventory. For many of people without access to the detailed unit-based emission inventory, it will be useful to see this information so that vertical distribution in the traditional inventories can also be improved.

Response:

In the simulation, the vertical distribution of point source emissions is calculated by employing a built-in plume-rise calculation algorithm of CMAQ based on the Briggs's scheme (Briggs, 1982). In this algorithm, plume rise is estimated by simulating the buoyancy effect and momentum rise, using hourly and gridded meteorological data. Then, the plume is distributed into the vertical layers that the plume intersects based on the pressure in each layer. (Page 5, Line 20-22; Page 8, Line 2-4)

The stack information required for plume rise calculation includes stack height, flue gas temperature, chimney diameter and flue gas velocity. For power plants, we get the stack height from Compilation of power industry statistics (China Electricity Council, 2015). For the stack height of cement factories, we refer to the emission standard of air pollutants for cement industry (Ministry of Environmental Protection of China, 2013). For the stack height of glass, brick, lime and ceramics industries, we refer to emission standard of air pollutants for industrial kiln and furnace (Ministry of Environmental Protection of China, 1997). For the stack height of non-ferrous metal smelter, coking, refinery and chemical industries, as well as the flue gas temperature, chimney diameter and flue gas velocity for all industrial sectors, we refer to the national information platform of pollutant discharge permit (http://114.251.10.126/permitExt/outside/default.jsp), where we can find very detailed information of the plants with the pollutant discharge permit. For the sources without the pollutant discharge permit, we use the parameters of the plant with a similar production output or coal consumption. (Page 5, Line 23 to Page 6, Line 5) The data source of stack information is shown in Table R1 (Table S5 in the manuscript).

Table R1 Data source of stack information

Sector	Stack height	Flue gas temperature, Chimney diameter, Flue gas velocity
Power plant	Compilation of power industry statistics	National information platform of pollutant discharge permit

Cement plant	Emission standard of air pollutants for cement industry
Glass, brick, lime and ceramics industries	Emission standard of air pollutants for industrial kiln and furnace
Non-ferrous metal smelter, coking, refinery and chemical industries	National information platform of pollutant discharge permit

The vertical distribution of emissions after plume rise for each industrial sector is shown in Table R2 (Table S6 in the manuscript). The empirical vertical distribution used for the proxy-based emission inventory is also provided for reference (Table R3, Table S7 in the manuscript). In general, compared with the proxy-based inventory, more emissions are distributed in higher vertical levels in the unit-based inventory with plume rise considered.

Table R2 Vertical distribution of emissions for each industrial sector in the unit-based inventory with plume rise considered

Layer	Sigma value	Level height (m)	Power plants		Iron plants		Cement plants		Industrial boilers		Industrial process	
			Jan	Jul	Jan	Jul	Jan	Jul	Jan	Jul	Jan	Jul
1	0.995	35	0%	0%	0%	0%	3%	3%	3%	4%	3%	6%
2	0.99	85	0%	0%	0%	0%	9%	11%	21%	21%	28%	31%
3	0.98	140	0%	0%	0%	6%	26%	32%	32%	41%	45%	36%
4	0.96	210	6%	9%	60%	85%	49%	49%	39%	31%	20%	24%
5	0.94	310	15%	17%	38%	9%	13%	5%	5%	2%	3%	3%
6	0.91	440	47%	45%	2%	0%	1%	0%	0%	0%	0%	0%
7	0.86	610	31%	29%	0%	0%	0%	0%	0%	0%	0%	0%

Table R3 Vertical distribution of emissions for each industrial sector in the proxy-based inventory

Layer	Sigma value	Level height (m)	Power plants	Iron plants	Cement plants	Industrial boilers	Industrial process
1	0.995	35	0%	6%	6%	50%	6%
2	0.99	85	10%	26%	26%	30%	26%
3	0.98	140	10%	68%	68%	20%	68%
4	0.96	210	30%	0%	0%	0%	0%
5	0.94	310	20%	0%	0%	0%	0%
6	0.91	440	20%	0%	0%	0%	0%
7	0.86	610	10%	0%	0%	0%	0%

To separate the contributions of horizontal and vertical distributions to the differences between the simulations using the proxy-based and unit-based inventories, we have conducted an additional simulation in which the unit-based inventory is used but the emission heights are assumed to be the same as the proxy-based inventory. The amount of emission is the same as the other two scenarios. We call the inventory used in this simulation “hypo unit-based inventory”.

Fig. R1 (Fig. 5 in the revised manuscript) shows the distribution of the monthly (January and July) mean concentrations of SO_2, NO_2, ozone, daily maximum 1-h averaged ozone, daily maximum 8-h averaged

ozone and $PM_{2.5}$ simulated with the proxy-based inventory, and the differences between the proxy-based simulation and the other two simulations (Diff1: hypo unit-based minus proxy-based; Diff2: unit-based minus proxy-based). For SO_2, NO_2 and $PM_{2.5}$, the concentrations in the urban area are generally higher with the proxy-based inventory than those with the unit-based inventory, especially in winter. In January, large concentration differences between simulations with two inventories are found in urban Tianjin, Tangshan, Baoding and Shijiazhuang, where a large amount of industrial emissions is allocated in the proxy-based inventory due to large population density. The simulation of July follows the same pattern but the concentrations and the difference between the concentrations with two inventories are lower than those of January. In some areas where many factories are located, such as the northern part of Xingtai city, the concentration with unit-based inventory is higher because of a high emission intensity. There are two reasons for the difference between results with proxy-based and unit-based inventories. The first one is the spatial distribution. With detailed information of industrial sectors, more emissions are allocated to certain locations in suburban/rural areas in the unit-based emission inventory. From "Diff1" (hypo unit-based minus proxy-based), we can see that the improved horizontal distribution of the unit-based emission inventory significantly decreases the $PM_{2.5}$, SO_2, and NO_2 concentrations in most urban centers, and significantly increases the concentrations in a large fraction of suburban and rural areas, especially the areas where large industrial plants are located in. The other reason is vertical distribution. Plume rise is calculated in the simulation with the unit-based inventory, which causes the difference of emissions in vertical layers. The higher the pollutants are emitted, the lower the ground concentration becomes. From the differences between Diff1 and Diff2 we can see that the plume rise leads to lower concentrations over the whole region. The results of the additional simulation have been added to the revised manuscript (Page 11, Line 6 to 26; Page 14, Line 2-4)

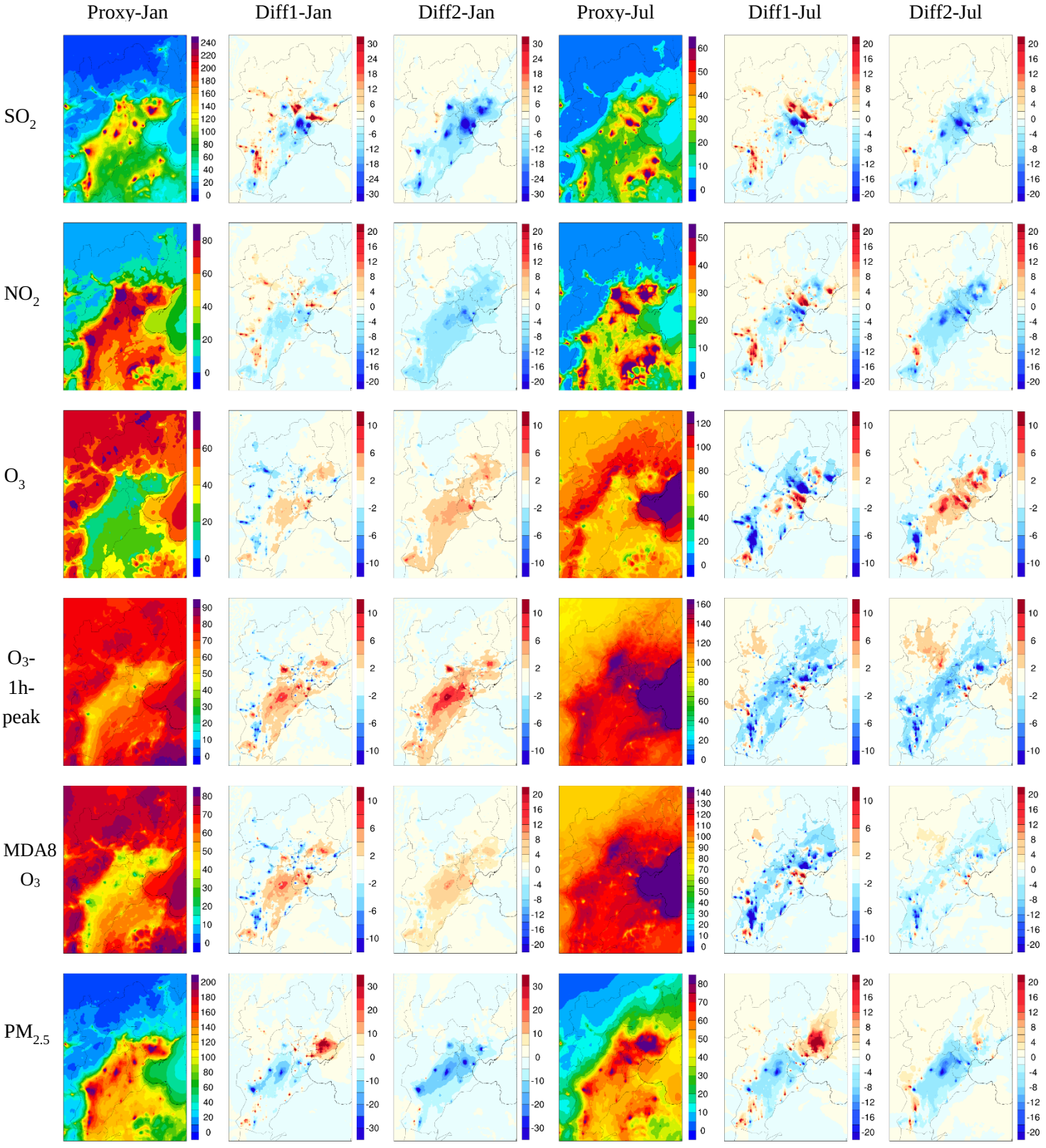

Fig. R1 Spatial distribution of the monthly (January and July) mean concentrations of SO_2, NO_2, ozone, daily maximum 1-h averaged ozone, daily maximum 8-h averaged ozone and $PM_{2.5}$ with the proxy-based inventory, and the differences between the other two simulations and proxy-based inventory (Diff1: hypo unit-based minus proxy-based; Diff2: unit-based minus proxy-based). The units are $\mu g/m^3$ for all panels.

(2) One of the major conclusions from the study is that unit-based emission inventory leads to significant improvement in the model performance. However, the only quantitative assessment is monthly average concentrations of SO2, NO2, O3, PM2.5 using all the stations in the domain. This is not sufficient as information is lost in the averaging process. At minimal, the authors should show performance of these pollutants at each individual sites. Time series should also be shown for sites with significant differences. It will help identify the cause of the differences. For O3, it is necessary to show performance of 1-hr peak ozone and 8-hr daily maximum. Very large error still exists for SO2. More discussion of this over-estimation should be included.

Response:

(1) Following the reviewer's comment, we summarize the model performance for major air pollutants at each individual site in Beijing (12 sites out of a total of 80 sites in the BTH region) in Table R1-R4 (Table S8-S11). The time series of $PM_{2.5}$ concentration at representative urban sites (Wanshouxigong and Dongsi) and suburban sites (Huairou and Shunyi) are shown in Fig. R2-R3 (Fig. S7-S8). For the urban sites, the concentrations of $PM_{2.5}$, SO_2 and NO_2 are much lower with the unit-based inventory than with the proxy-based inventory. For the suburban sites, however, the concentrations are either slightly higher or slightly lower with the unit-based inventory than with the proxy-based inventory. The situation for ozone is quite the opposite. The ozone concentration at urban sites is higher with the unit-based inventory than with the proxy-based inventory. In suburban sites, it is lower with the unit-based inventory than with the proxy-based inventory. In addition, for the simulations with the unit-based inventory, the normalized mean error (NME) and mean fractional error (MFE) of individual sites are usually lower than those with the proxy-based inventory while the correlation efficient is usually higher, which means that the error is generally smaller and the trend is more similar to the observation when the unit-based inventory is used.

(2) The figures of time series of $PM_{2.5}$ concentration corroborates the preceding conclusion. At urban sites, the concentration with the unit-based inventory is substantially lower than that with the proxy-based inventory throughout the simulation periods. For suburban sites, the concentration is slightly lower with the unit-based inventory than that with the proxy-based inventory in most of the simulation period.

(3) To further quantify the impact of changed emission distribution between urban and suburban areas, we introduced the metric of "concentration gradient", which is defined as the ratios of urban concentrations to suburban concentrations. As shown in Fig. 6 in the manuscript, the concentration gradients simulated with the unit-based inventory agree much better with observations than those simulated with the proxy-based inventory, implying that the unit-based emission inventory better reproduces the distributions of pollutant emissions between the urban and suburban areas.

The preceding tables, figures, and descriptions have been added to the revised manuscript. (Page 12, Line 5-22)

(4) For ozone, the performance statistics for 1-hr peak ozone and 8-hr daily maximum concentration have been calculated, which is shown in Table 2 in the manuscript.

(5) The overestimation of SO_2 concentrations may be due to the lack of several SO_2 reaction mechanisms in CMAQ, such as heterogeneous reactions of SO_2 on the surface of dust particles (Fu et al., 2016), the oxidation of SO_2 by NOx in aerosol liquid water (Cheng et al., 2016;Wang et al., 2016), the effects of SO_2 and NH_3 on secondary organic aerosol formation (Chu et al., 2016), etc. The biased

spatial distribution of SO_2 emissions from residential combustion may also contribute to the overestimation. A large fraction of residential combustion takes place in the rural areas. In this work, however, the emission of residential combustion is allocated by GDP and population, which leads to an overestimation of SO_2 emission in urban area and hence an overestimation of SO_2 concentration. (Page 10, Line 4-11)

Table R4 The statistics for model performance of $PM_{2.5}$ with proxy-based and unit-based inventories

Months	Sites	Concentration (μg/m^3)			NMB		NME		MFB		MFE		R	
		proxy-based	unit-based	OBS	proxy-based	unit-based	proxy-based	unit-based	proxy-based	unit-based	proxy-based	unit-based	proxy-based	unit-based
Jan	Wanshouxigong	111.2	88.0	108.4	3%	-19%	54%	49%	20%	-3%	62%	60%	0.58	0.60
	Dingling Tomb	36.8	36.9	69.3	-47%	-47%	54%	53%	-59%	-55%	72%	68%	0.67	0.68
	Dongsi	112.2	91.6	104.1	8%	-12%	58%	51%	24%	6%	64%	61%	0.55	0.56
	Heaven Temple	110.7	90.3	97.6	13%	-8%	58%	51%	31%	10%	64%	61%	0.59	0.60
	Nongzhanguan	92.6	77.7	101.9	-9%	-24%	52%	50%	4%	-10%	59%	58%	0.57	0.59
	Guanyuan	110.5	86.4	100.6	10%	-14%	60%	51%	23%	1%	65%	61%	0.55	0.56
	Haidian	86.8	70.0	109.3	-21%	-36%	55%	53%	-17%	-35%	66%	67%	0.53	0.54
	Shunyi	89.4	83.3	92.3	-3%	-10%	56%	54%	8%	3%	62%	61%	0.55	0.55
	Huairou	49.8	48.5	86.9	-43%	-44%	57%	55%	-71%	-69%	86%	82%	0.61	0.62
	Changping	74.7	70.3	85.6	-13%	-18%	54%	51%	-4%	-8%	58%	56%	0.57	0.58
	Olympic center	93.6	82.5	94.8	-1%	-13%	56%	50%	9%	1%	62%	59%	0.57	0.59
	Gucheng	77.0	63.2	102.0	-25%	-38%	50%	51%	-19%	-37%	60%	64%	0.59	0.60
Jul	Wanshouxigong	55.7	50.0	96.4	-42%	-48%	55%	58%	-51%	-61%	69%	75%	0.53	0.52
	Dingling Tomb	24.6	26.1	83.7	-71%	-69%	74%	72%	-106%	-102%	112%	109%	0.55	0.57
	Dongsi	57.3	52.2	110.0	-48%	-53%	57%	59%	-54%	-61%	72%	75%	0.56	0.55
	Heaven Temple	58.0	52.5	103.3	-44%	-49%	56%	58%	-52%	-61%	70%	74%	0.51	0.50
	Nongzhanguan	54.4	50.2	91.7	-41%	-45%	54%	55%	-54%	-59%	70%	72%	0.50	0.50
	Guanyuan	54.8	49.8	99.6	-45%	-50%	55%	57%	-59%	-67%	73%	78%	0.56	0.56
	Haidian	42.8	39.9	99.8	-57%	-60%	61%	63%	-88%	-91%	93%	95%	0.60	0.60
	Shunyi	60.2	55.8	101.7	-41%	-45%	54%	55%	-41%	-47%	67%	70%	0.58	0.57
	Huairou	44.8	45.0	101.2	-56%	-56%	60%	59%	-89%	-78%	96%	85%	0.68	0.68
	Changping	37.2	39.0	91.9	-60%	-58%	65%	63%	-77%	-74%	86%	84%	0.65	0.67
	Olympic center	50.5	47.1	104.8	-52%	-55%	57%	59%	-73%	-77%	81%	83%	0.60	0.59
	Gucheng	38.2	36.9	97.2	-61%	-62%	63%	64%	-96%	-98%	99%	100%	0.64	0.63

Table R5 The statistics for model performance of NO_2 with proxy-based and unit-based inventories

Months	Sites	Concentration (μg/m^3)			NMB		NME		MFB		MFE		R	
		proxy-based	unit-based	OBS	proxy-based	unit-based	proxy-based	unit-based	proxy-based	unit-based	proxy-based	unit-based	proxy-based	unit-based
Jan	Wanshouxigong	135.3	96.0	81.1	67%	18%	81%	47%	43%	11%	59%	46%	0.60	0.64
	Dingling Tomb	39.9	41.4	37.2	7%	11%	60%	58%	4%	11%	60%	60%	0.64	0.66
	Dongsi	135.1	101.4	66.3	104%	53%	116%	75%	59%	37%	72%	60%	0.43	0.42
	Heaven Temple	134.9	101.8	73.4	84%	39%	94%	61%	48%	21%	60%	50%	0.57	0.58
	Nongzhanguan	108.0	93.9	68.0	59%	38%	79%	59%	33%	26%	58%	51%	0.60	0.63
	Guanyuan	141.7	99.9	76.1	86%	31%	103%	61%	42%	12%	63%	52%	0.59	0.59
	Haidian	106.1	80.0	93.5	13%	-14%	66%	50%	-12%	-32%	62%	60%	0.47	0.48
	Shunyi	100.7	92.7	56.8	77%	63%	93%	80%	42%	37%	62%	58%	0.61	0.61
	Huairou	54.8	54.0	56.7	-3%	-5%	72%	68%	-45%	-41%	85%	81%	0.55	0.57
	Changping	102.3	95.3	57.0	80%	67%	98%	87%	39%	34%	60%	57%	0.54	0.56
	Olympic center	113.9	100.0	67.7	68%	48%	86%	66%	43%	37%	63%	58%	0.60	0.62
	Gucheng	95.0	73.6	75.9	25%	-3%	61%	46%	12%	-9%	55%	52%	0.61	0.64
Jul	Wanshouxigong	22.1	18.4	41.3	-46%	-56%	59%	62%	-72%	-86%	83%	92%	0.17	0.15
	Dingling Tomb	5.7	7.2	17.1	-67%	-58%	70%	63%	-116%	-102%	118%	106%	0.34	0.37
	Dongsi	25.6	22.6	43.5	-41%	-48%	57%	58%	-65%	-72%	78%	81%	0.22	0.19
	Heaven Temple	24.5	21.0	36.4	-33%	-42%	56%	56%	-53%	-63%	73%	77%	0.24	0.21
	Nongzhanguan	22.8	21.7	44.9	-49%	-52%	60%	60%	-78%	-77%	87%	84%	0.27	0.27
	Guanyuan	21.4	18.1	42.2	-49%	-57%	61%	62%	-75%	-87%	86%	93%	0.11	0.12
	Haidian	14.9	13.7	54.3	-73%	-75%	74%	76%	-119%	-123%	121%	124%	0.07	0.09
	Shunyi	21.6	19.7	28.1	-23%	-30%	39%	41%	-36%	-43%	54%	57%	0.66	0.64
	Huairou	11.9	12.8	25.0	-52%	-49%	62%	60%	-96%	-86%	105%	95%	0.39	0.40
	Changping	15.1	17.1	32.5	-53%	-47%	58%	54%	-85%	-75%	90%	81%	0.27	0.28
	Olympic center	20.1	18.5	48.6	-59%	-62%	64%	64%	-93%	-96%	97%	99%	0.23	0.25
	Gucheng	12.4	12.2	45.6	-73%	-73%	74%	74%	-118%	-118%	119%	118%	0.23	0.24

Table R6 The statistics for model performance of SO_2 with proxy-based and unit-based inventories

Months	Sites	Concentration (μg/m^3)			NMB		NME		MFB		MFE		R	
		proxy-based	unit-based	OBS	proxy-based	unit-based	proxy-based	unit-based	proxy-based	unit-based	proxy-based	unit-based	proxy-based	unit-based
Jan	Wanshouxigong	102.2	93.4	62.0	65%	51%	77%	67%	60%	51%	69%	65%	0.51	0.51
	Dingling Tomb	36.0	36.7	35.4	2%	3%	73%	71%	-9%	-4%	70%	69%	0.43	0.44
	Dongsi	99.8	91.8	56.7	76%	62%	86%	75%	64%	57%	72%	67%	0.52	0.53
	Heaven Temple	99.7	92.0	47.1	112%	95%	124%	112%	81%	74%	88%	84%	0.30	0.30
	Nongzhanguan	88.0	82.7	58.9	50%	40%	69%	62%	49%	45%	64%	61%	0.50	0.52
	Guanyuan	101.2	91.6	54.8	85%	67%	97%	84%	67%	58%	77%	72%	0.51	0.51
	Haidian	89.7	81.7	58.2	54%	40%	81%	73%	48%	40%	72%	70%	0.47	0.46
	Shunyi	68.9	66.1	44.0	57%	50%	79%	75%	56%	53%	73%	71%	0.48	0.47
	Huairou	46.3	46.5	45.6	2%	2%	66%	63%	-8%	-4%	74%	71%	0.40	0.40
	Changping	66.3	64.0	57.6	15%	11%	58%	56%	12%	8%	56%	56%	0.46	0.46
	Olympic center	87.2	82.6	58.3	50%	42%	72%	66%	45%	42%	65%	62%	0.50	0.50
	Gucheng	80.6	72.4	52.9	52%	37%	79%	69%	47%	38%	71%	66%	0.52	0.52
Jul	Wanshouxigong	69.9	66.5	5.6	1144%	1083%	1168%	1110%	149%	145%	156%	153%	-0.31	-0.31
	Dingling Tomb	9.7	10.5	4.6	112%	128%	168%	178%	52%	58%	97%	98%	0.12	0.11
	Dongsi	74.6	71.8	9.6	680%	650%	696%	669%	135%	133%	141%	141%	-0.05	-0.06
	Heaven Temple	67.3	64.0	7.4	805%	762%	831%	790%	136%	133%	146%	144%	-0.27	-0.28
	Nongzhanguan	62.9	61.0	8.7	622%	600%	649%	627%	127%	128%	137%	138%	-0.07	-0.08
	Guanyuan	77.0	73.5	8.5	802%	761%	842%	802%	149%	147%	155%	153%	0.04	0.04
	Haidian	62.5	60.2	12.2	413%	394%	444%	424%	96%	95%	122%	120%	-0.26	-0.26
	Shunyi	36.8	33.5	6.5	463%	412%	498%	454%	112%	106%	130%	128%	-0.13	-0.15
	Huairou	22.9	23.7	4.5	405%	422%	435%	451%	112%	119%	126%	129%	-0.01	-0.02
	Changping	28.2	30.6	5.4	421%	466%	457%	493%	114%	122%	127%	133%	-0.06	-0.02
	Olympic center	64.2	61.8	5.0	1174%	1127%	1193%	1147%	141%	140%	149%	149%	-0.09	-0.08
	Gucheng	44.1	43.0	5.2	741%	720%	767%	744%	128%	128%	140%	139%	-0.19	-0.17

Table R7 The statistics for model performance of ozone with proxy-based and unit-based inventories

Months	Sites	Concentration (μg/m^3)			NMB		NME		MFB		MFE		R	
		proxy-based	unit-based	OBS	proxy-based	unit-based	proxy-based	unit-based	proxy-based	unit-based	proxy-based	unit-based	proxy-based	unit-based
Jan	Wanshouxigong	11.0	14.0	12.0	-8%	17%	100%	115%	-86%	-71%	153%	149%	0.43	0.40
	Dingling Tomb	47.2	46.4	35.4	33%	31%	56%	54%	20%	21%	80%	78%	0.60	0.61
	Dongsi	12.0	14.7	23.3	-49%	-37%	71%	75%	-116%	-106%	139%	137%	0.50	0.44
	Heaven Temple	11.5	14.2	20.8	-45%	-32%	76%	82%	-108%	-97%	144%	143%	0.46	0.41
	Nongzhanguan	15.9	17.5	20.9	-24%	-16%	67%	69%	-87%	-80%	128%	127%	0.61	0.59
	Guanyuan	12.6	16.1	16.0	-21%	1%	82%	94%	-78%	-62%	144%	142%	0.50	0.43
	Haidian	18.3	22.8	14.9	23%	54%	99%	122%	-48%	-34%	139%	138%	0.53	0.42
	Shunyi	20.4	21.3	22.9	-11%	-7%	57%	57%	-66%	-59%	116%	113%	0.71	0.70
	Huairou	40.8	40.2	26.2	56%	53%	87%	86%	13%	13%	101%	100%	0.53	0.52
	Changping	26.9	28.1	25.9	4%	9%	55%	55%	-34%	-28%	90%	89%	0.65	0.65
	Olympic center	17.2	18.5	15.6	10%	18%	84%	92%	-50%	-47%	136%	136%	0.58	0.52
	Gucheng	20.6	25.1	31.5	-35%	-20%	64%	65%	-84%	-64%	112%	105%	0.51	0.47
Jul	Wanshouxigong	57.8	58.5	104.8	-45%	-44%	55%	55%	-89%	-86%	104%	102%	0.63	0.62
	Dingling Tomb	106.6	107.4	115.2	-7%	-7%	40%	38%	1%	1%	40%	39%	0.49	0.56
	Dongsi	55.1	55.5	92.8	-41%	-40%	57%	57%	-82%	-80%	104%	102%	0.55	0.54
	Heaven Temple	58.6	59.0	101.3	-42%	-42%	55%	55%	-82%	-78%	102%	99%	0.63	0.61
	Nongzhanguan	63.4	63.1	107.0	-41%	-41%	57%	57%	-58%	-57%	99%	98%	0.56	0.56
	Guanyuan	56.5	57.3	98.7	-43%	-42%	61%	61%	-79%	-77%	107%	105%	0.52	0.52
	Haidian	68.5	69.3	83.4	-18%	-17%	58%	57%	-28%	-26%	93%	92%	0.54	0.55
	Shunyi	70.2	71.2	101.9	-31%	-30%	44%	44%	-37%	-33%	63%	61%	0.70	0.69
	Huairou	92.8	91.1	112.0	-17%	-19%	41%	41%	-12%	-14%	46%	46%	0.54	0.54
	Changping	91.4	90.1	115.3	-21%	-22%	44%	42%	-17%	-18%	52%	51%	0.51	0.55
	Olympic center	64.3	64.7	90.3	-29%	-28%	59%	59%	-45%	-43%	99%	97%	0.52	0.52
	Gucheng	80.5	80.4	100.4	-20%	-20%	51%	50%	-15%	-15%	73%	72%	0.58	0.59

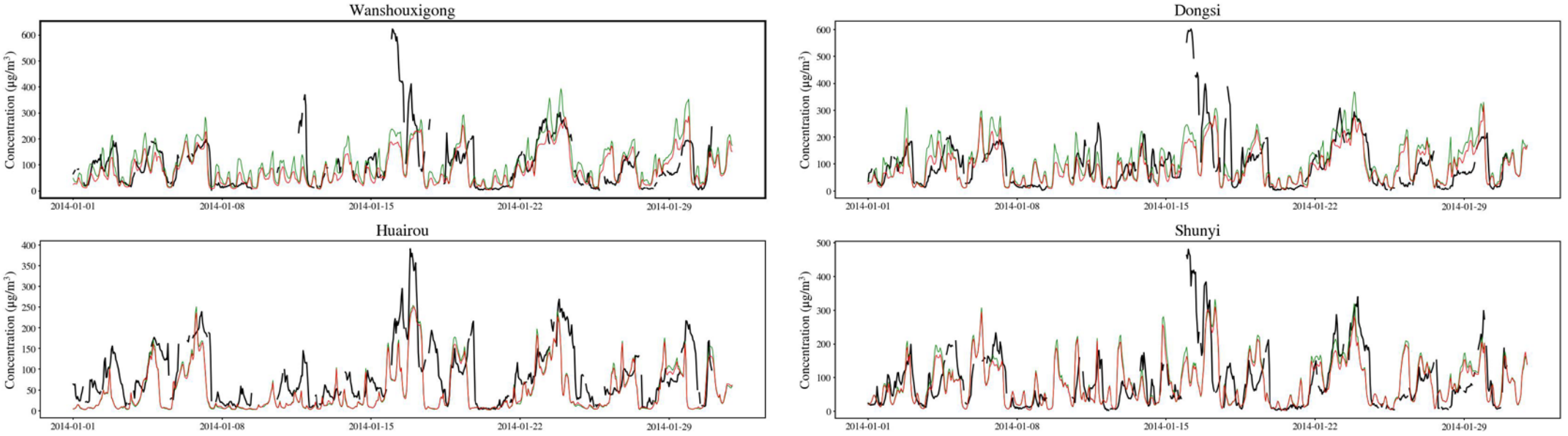

Fig. R2 The $PM_{2.5}$ concentration in January in Beijing (The black, green and red lines represent observation, results with proxy-based and unit-based inventories)

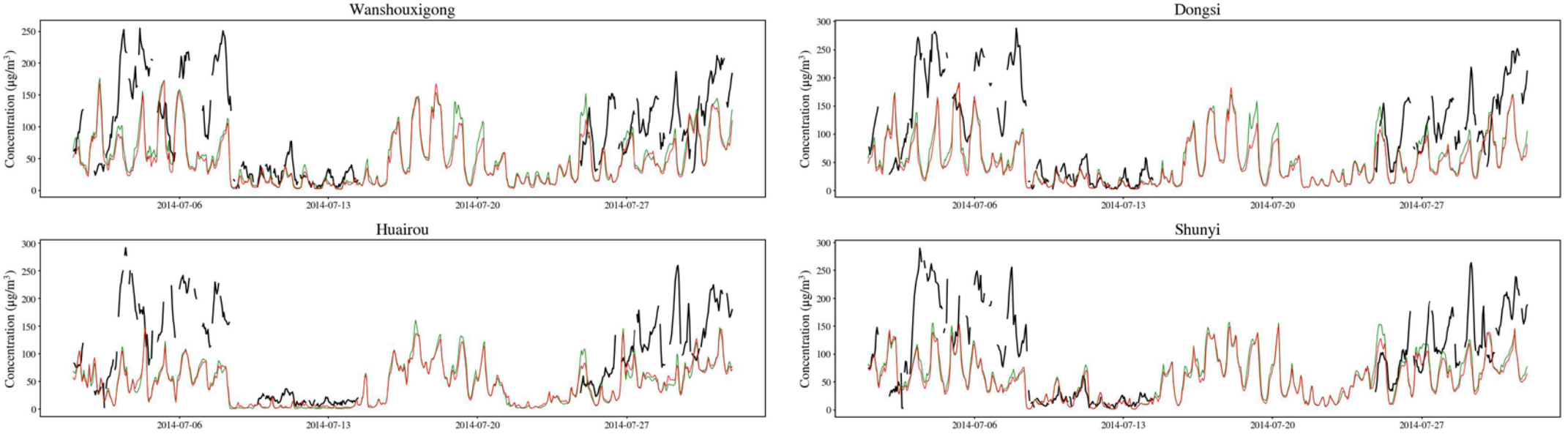

Fig. R3 The $PM_{2.5}$ concentration in July in Beijing

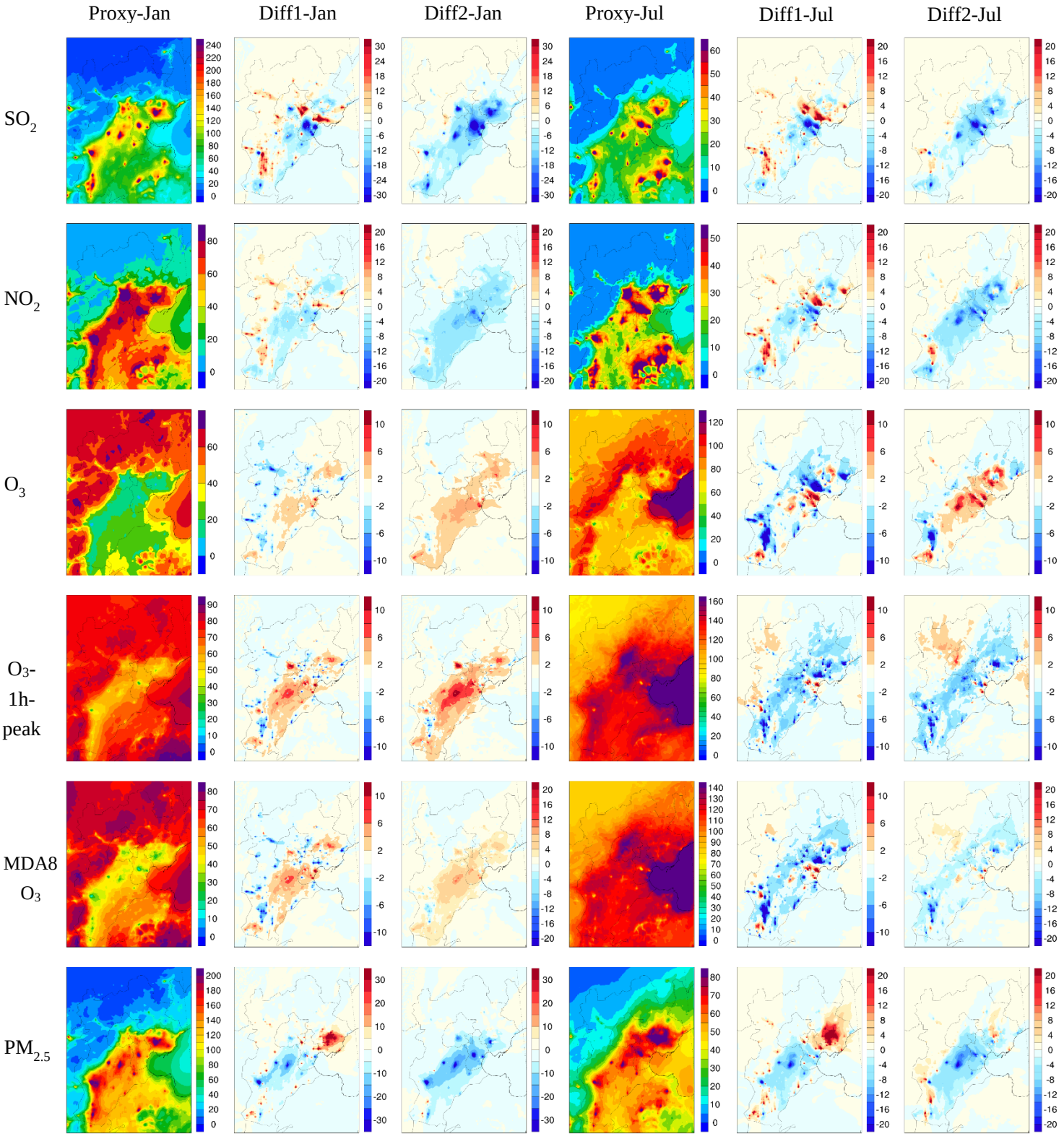

Fig. R4 Spatial distribution of the monthly (January and July) mean concentrations of SO_2, NO_2, ozone, 1h-peak ozone, MDA8 ozone and $PM_{2.5}$ with the proxy-based inventory, and the differences between the other two simulations and proxy-based inventory (Diff1: hypo unit-based minus proxy-based; Diff2: unit-based minus proxy-based). The units are $\boldsymbol{\mu g/m^3}$ for all panels.

(3) Table 1 shows "annual average" but only January and July simulations were performed. How did you calculate annual average with only two months of simulation?

Response: We revised "annual average" to “two-month average” in the revised manuscript. (Table 1)

References:

Briggs, G. A.: Plume Rise Predictions, in: Lectures on Air Pollution and Environmental Impact Analyses, edited by: Haugen, D. A., American Meteorological Society, Boston, MA, 59-111, 1982.

Cheng, Y., Zheng, G., Wei, C., Mu, Q., Zheng, B., Wang, Z., Gao, M., Zhang, Q., He, K., Carmichael, G., Poschl, U., and Su, H.: Reactive nitrogen chemistry in aerosol water as a source of sulfate during haze events in China, Science Advances, 2, 10.1126/sciadv.1601530, 2016.

China Electricity Council: Compilation of power industry statistics 2014, China Electricity Council, Beijing, 2015.

Chu, B., Zhang, X., Liu, Y., He, H., Sun, Y., Jiang, J., Li, J., and Hao, J.: Synergetic formation of secondary inorganic and organic aerosol: effect of SO₂ and NH₃ on particle formation and growth, Atmos Chem Phys, 16, 14219-14230, 10.5194/acp-16-14219-2016, 2016.

Fu, X., Wang, S., Chang, X., Cai, S., Xing, J., and Hao, J.: Modeling analysis of secondary inorganic aerosols over China: pollution characteristics, and meteorological and dust impacts, Sci Rep, 6, 35992, 10.1038/srep35992, 2016.

Ministry of Environmental Protection of China: Emission standard of air pollutants for industrial kiln and furnace, Ministry of Environmental Protection of China (MEP), Beijing, 1997.

Ministry of Environmental Protection of China: Emission standard of air pollutants for cement industry, Ministry of Environmental Protection of China (MEP), Beijing, 2013.

Wang, G., Zhang, R., Gomez, M. E., Yang, L., Levy Zamora, M., Hu, M., Lin, Y., Peng, J., Guo, S., Meng, J., Li, J., Cheng, C., Hu, T., Ren, Y., Wang, Y., Gao, J., Cao, J., An, Z., Zhou, W., Li, G., Wang, J., Tian, P., Marrero-Ortiz, W., Secrest, J., Du, Z., Zheng, J., Shang, D., Zeng, L., Shao, M., Wang, W., Huang, Y., Wang, Y., Zhu, Y., Li, Y., Hu, J., Pan, B., Cai, L., Cheng, Y., Ji, Y., Zhang, F., Rosenfeld, D., Liss, P. S., Duce, R. A., Kolb, C. E., and Molina, M. J.: Persistent sulfate formation from London Fog to Chinese haze, Proc Natl Acad Sci U S A, 10.1073/pnas.1616540113, 2016.

Development of a unit-based industrial emission inventory in the Beijing-Tianjin-Hebei region and resulting improvement in air quality modelling

Haotian Zheng[a,b 1], Siyi Cai[a, 1], Shuxiao Wang[a,b*], Bin Zhao[c*], Xing Chang[a,b], Jiming Hao[a,b]

[a] State Key Joint Laboratory of Environmental Simulation and Pollution Control, School of Environment, Tsinghua University, Beijing, 100084, China

[b] State Environmental Protection Key Laboratory of Sources and Control of Air Pollution Complex, Beijing 100084, China

[c]Joint Institute for Regional Earth System Science and Engineering and Department of Atmospheric and Oceanic Sciences, University of California, Los Angeles, CA 90095, USA

Correspondence to: S. Wang (shxwang@tsinghua.edu.cn) and B. Zhao (zhaob1206@ucla.edu)

[1] These authors contributed equally to this study.

Abstract.

The Beijing-Tianjin-Hebei (BTH) region is a metropolitan area with the most severe fine particle ($PM_{2.5}$) pollution in China. Accurate emission inventory plays an important role in air pollution control policy making. In this study, we develop a unit-based emission inventory for industrial sectors in the BTH region, including power plants, industrial boilers, steel, non-ferrous metal, coking, cement, glass, brick, lime, ceramics, refinery, and chemical industries, based on detailed information for each enterprise, such as location, annual production, production technology/process and air pollution control facilities. In the BTH region, the emissions of sulfur dioxide (SO_2), nitrogen oxide (NO_x), particulate matter with diameter less than 10 μm (PM_{10}), $PM_{2.5}$, black carbon (BC), organic carbon (OC), and non-methane volatile organic compounds (NMVOCs) from industrial sectors are 869 kt, 1164 kt, 910 kt, 622 kt, 71 kt, 63 kt and 1390 kt in 2014, respectively, accounting for 61%, 55%, 62%, 56%, 58%, 22% and 36%, respectively, of the total emissions. Compared with the traditional proxy-based emission inventory, much less emissions in the high-resolution unit-based inventory are allocated to the urban center because of the accurate positioning of industrial enterprises. We apply the Community Multi-scale Air Quality (CMAQ) model

simulation to evaluate the unit-based inventory. The simulation results show that the unit-based emission inventory gives better performance of both $PM_{2.5}$ and gaseous pollutants than the proxy-based emission inventory. The normalized mean biases (NMBs) are 81%, 21%, 1% and -7% for concentrations of SO_2, NO_2, ozone and $PM_{2.5}$, respectively, with the unit-based inventory, in contrast to 124%, 39%, -8% and 9% with the proxy-based inventory. Furthermore, the concentration gradients of $PM_{2.5}$, which are defined as the ratio of urban concentration to suburban concentration, are 1.6, 2.1 and 1.5 in January and 1.3, 1.5 and 1.3 in July, for simulations with the unit-based inventory, simulations with the proxy-based inventory, and observations, respectively, in Beijing. For ozone, the corresponding gradients are 0.7, 0.5 and 0.9 in January and 0.9, 0.8 and 1.1 in July, implying that the unit-based emission inventory better reproduces the distributions of pollutant emissions between the urban and suburban areas.

1 Introduction

The Beijing-Tianjin-Hebei (BTH) region is the political, economic and cultural center of China. According to China National Environmental Monitoring Centre (data source: http://106.37.208.233:20035/), in 2017, the annual average concentration of $PM_{2.5}$ in Beijing, Tianjin and Hebei are 65.6, 63.8 and 57.1 $\mu g/m^3$, ranking second, third and sixth among all provinces. The severe $PM_{2.5}$ pollution in the BTH region is largely attributed to the substantial emissions of air pollutants (Zhao et al., 2017a). An accurate emission inventory, in terms of both emission rates and spatial distribution, is imperative for an adequate understanding of the sources and formation mechanism of the serious air pollution.

The spatial distribution is one of the most uncertain component of emission inventories considering the diverse source categories and complex emission characteristics. The traditional method of spatial allocation is to distribute the emissions by administrative region into grids based on spatial proxies such as population, gross domestic product (GDP), road map, land use data and nighttime lights (Geng et al., 2017;Oda and Maksyutov, 2011;Streets et al., 2003). The results may deviate significantly from the actual spatial distributions of many sources (Zhou and Gurney, 2011), especially the power and industrial

sources, which contribute over 50% of the total $PM_{2.5}$ emissions in China (Zhao et al., 2013a). Due to the stricter air quality regulation and higher land price in urban area, people tend to build factories in suburban area where the population density and GDP are lower. Zheng et al. (2017) studied the influence of the resolution of gridded emission inventory and found that there were large biases when the inventory was distributed to very fine resolution following the traditional proxy-based allocation method. The emission inventory could be significantly improved with detailed information of point sources such as power plants, steel plants, cement plants, etc. The high spatial resolution of the inventory may subsequently improve the air quality modelling results and enable a better source apportionment of air pollution (Zhao et al., 2017c).

A couple of studies have developed the emission inventory in the BTH region (Li et al., 2017;Wang et al., 2014), and some others have provided emission estimates for this region as part of national or larger-scale emission inventories (Ohara et al., 2007;Stohl et al., 2015). However, only limited studies estimated the emissions by individual point sources (i.e., unit-based emission inventory). Zhao et al. (2008), Chen et al. (2014) and Liu et al. (2015) established unit-based emission inventories of coal-fired power plants in China. Wang et al. (2016b) and Wu et al. (2015) developed an emission inventory of steel industry. Lei et al. (2011) and Chen et al. (2015) established an emission inventory of cement industry in China. Qi et al. (2017) established an emission inventory in BTH region with power and major industrial sources treated as point sources. These studies usually focused on one or several major industries, and did not cover all industrial sectors in the BTH region. Moreover, these previous studies seldom validated the unit-based emission inventory or evaluated the improvement it brings to air quality simulation.

In this study, we developed a unit-based emission inventory of industrial sectors for the Beijing-Tianjin-Hebei region. A three-domain nested simulation by WRF-CMAQ model was applied to evaluate the emission inventory. In order to study the influence of the point sources, we compared the simulation results of this emission inventory with those of a traditional proxy-based emission inventory.

2 Materials and methods

2.1 High-resolution emission inventory for Beijing-Tianjin-Hebei region

A unit-based method is applied to quantify the emissions from industrial sectors such as power plant, industrial boiler, iron and steel production, non-ferrous metal smelter, coking, cement, glass, brick, lime, ceramics, refinery, and chemical industries in 2014. The product yields used for estimating emissions of each sector are shown in SI. The pollutant emissions from each industrial enterprise are calculated from activity level (energy consumption for power plants and industrial boilers, and product yield for other sectors), emission factor, and removal efficiency of control technology, as shown in the following equation:

$$\boldsymbol{E_{i,j} = A_j \times EF_{i,j} \times \left(1 - \eta_{i,j}\right)} \quad (1)$$

where $\boldsymbol{E_{i,j}}$ is emissions of pollutant i from industrial enterprise j, $\boldsymbol{A_j}$ is activity level of industrial enterprise j, $\boldsymbol{EF_{i,j}}$ is uncontrolled emission factor of pollutant i from industrial enterprise j, and $\boldsymbol{\eta_{i,j}}$ is removal efficiency of pollutant i by control technology in enterprise j. $\boldsymbol{\eta_{i,j}}$ is determined by the production process and control technology of the industrial enterprise. The $\boldsymbol{EF_{i,j}}$, which depends on the production process of the industrial enterprise, are calculated according to the sulfur and ash contents of fuels (e.g. coal) used in each province (for PM and SO_2), or obtained from our previous study (Zhao et al., 2013b) (for other pollutants).

For those industrial sources with multiple production processes, such as iron and steel production and cement production, emissions are calculated by using the following equation:

$$\boldsymbol{E_{i,j} = \sum_m \left(AK_{j,m} \times EF_{i,m} \times \left(1 - \eta_{i,j,m}\right)\right) + \left(AC_j \times ef_i \times \left(1 - \eta_{i,j}\right)\right)} \quad (2)$$

where $\boldsymbol{E_{i,j}}$ is emissions of pollutant i from industrial enterprise j, $\boldsymbol{AK_{j,m}}$ is the amount of clinker produced by the clinker burning process m of the enterprise j, $\boldsymbol{EF_{i,m}}$ is uncontrolled emission factor for pollutant i from the clinker burning process m, $\boldsymbol{\eta_{i,j,m}}$ is removal efficiency of pollutant i from the clinker burning process m in enterprise j, $\boldsymbol{AC_j}$ is the amount of cement produced by enterprise j, $\boldsymbol{ef_i}$ is uncontrolled emission factors from the clinker processing stage ($\boldsymbol{ef_i}$=0 if i is not particulate matter), $\boldsymbol{\eta_{i,j}}$ is removal

efficiency of pollutant i in enterprise j. $\eta_{i,j,m}$ and $\eta_{i,j}$ both depend on the control technology of the industrial enterprise.

The production processes represented by the first and second terms of equation (2) are frequently performed in different enterprises. For example, for cement production, clinker may be produced in one enterprise and subsequently processed in another enterprise, which is very common.

For all power and industrial sources except industrial boilers, we collect their detailed information, including latitude/longitude, annual product, production technology/process, and pollution control facilities from compilation of power industry statistics (China Electricity Council, 2015a), China Iron and Steel Industry Association (http://www.chinaisa.org.cn), China Cement Association (http://www.chinacca.org), Chinese environmental statistics (collected from provincial environmental protection bureaus), the first national census of pollution sources (National Bureau of Statistics (NBS), 2010) and bulletin of desulfurization and denitrification facilities from Ministry of Ecology and Environment of China (http://www.mee.gov.cn). These emission sources include 242 power plants, 333 iron and steel plants, 639 cement plants, 151 nonferrous metal smelters, 211 lime plants, 1222 brick and tile plants, 37 ceramic plants, 42 glass plants, 106 coking plants, 21 refinery plants, and 328 chemical plants. The iron and cement sectors are divided to specific industrial processes. For industrial boilers, we obtained the location, fuel use amount, and control technologies of over 8 thousand industrial boilers in Beijing, Tianjin, and Hebei from Xue et al. (2016), Tianjin Environmental Protection Bureau, and Hebei Environmental Protection Bureau.

Plume rise is caused by buoyancy effect and momentum rise (Briggs, 1982). Therefore, the stack information including stack height, flue gas temperature, chimney diameter and flue gas velocity is essential for plume rise calculation. For power plants, we get the stack height from Compilation of power industry statistics (China Electricity Council, 2015a). For the stack height of cement factories, we refer to the emission standard of air pollutants for cement industry (Ministry of Environmental Protection of China, 2013). For the stack height of glass, brick, lime and ceramics industries, we refer to emission standard of air pollutants for industrial kiln and furnace (Ministry of Environmental Protection of China, 1997). For the stack height of non-ferrous metal smelter, coking, refinery and chemical industries, as well

as the flue gas temperature, chimney diameter and flue gas velocity for all industrial sectors, we refer to the national information platform of pollutant discharge permit (http://114.251.10.126/permitExt/outside/default.jsp), where we can find very detailed information of the plants with the pollutant discharge permit. For the sources without the pollutant discharge permit, we use the parameters of the plant with a similar production output or coal consumption.

The emission inventory for other sources, including residential sources, transportation, solvent use, and open burning, is developed based on the "top-down method" following our previous work (Fu et al., 2013;Wang et al., 2014;Zhao et al., 2013b). The method is the same as **Eq (1)** except that the emissions are calculated for individual prefecture-level city rather than individual enterprise. The activity data and technology distribution for each sector are derived based on the Statistics Yearbook (Beijing Municipal Bureau of Statistics, 2015;Hebei Municipal Bureau of Statistics, 2015;National Bureau of Statistics (NBS), 2015b, c, d, e, f, g, h, i, j, a;Tianjin Municipal Bureau of Statistics, 2015), a wide variety of Chinese technology reports (China Electricity Council, 2015b;National Bureau of Statistics (NBS), 2012), and an energy demand modelling approach. **Fig.S1** shows energy consumption in the BTH region in 2014. We compared the sum of the energy consumption for each plant with the energy statistics. The sum of individual plants accounts for over 90% of the energy consumption or product yield reported in the statistics. For the plants not included in the preceding data sources, we calculate the emission by using "top-down method". The emission factors are also obtained from Zhao et al. (2013b). The speciation of $PM_{2.5}$ in both inventories is from Fu et al. (2013) while the speciation of NMVOCs is updated by Wu et al. (2017). The penetrations of removal technologies are obtained from the evolution of emission standards and a variety of technical reports (Chinese State Council, 2013).

2.2 Air quality model configuration

In this work, we use CMAQ version 5.0.2 (EPA, 2014) to simulate the concentration of pollutants. A three-domain nested simulation is established as shown in **Fig. 1** (left). The first domain covers almost entire area of China, Korea, Japan, and parts of India and Southeast Asia with a horizontal grid resolution of 36 km × 36 km. The second domain covers eastern China with a resolution of 12 km × 12 km. The

third domain with a horizontal resolution of 4 km × 4 km focuses on the Beijing-Tianjin-Hebei region. The observational sites in Beijing-Tianjin-Hebei region are marked in **Fig. 1** (right). All of the grids are divided to 14 layers vertically from surface to an altitude of about 19 km above the ground and the thickness of the first layer is about 40 m.

In order to minimize the influence of initial condition, we choose 5 days of spin-up period. The Carbon Bond 05 (CB05) and AERO6 (Sarwar et al., 2011) are chosen as the gas-phase and aerosol chemical mechanisms, respectively. The simulation periods are January and July of 2014, representing winter and summer, respectively.

We use the Weather Research and Forecasting (WRF) model version 3.7.1 (Skamarock et al., 2008) to simulate the meteorological fields. The physics options for the WRF simulation are the Kain-Fritsch cumulus scheme (Kain, 2004), the Morrison double-moment scheme for cloud microphysics (Morrison et al., 2005), the Pleim-Xiu land surface model (Xiu and Pleim, 2001), Pleim-Xiu surface layer scheme (Pleim, 2006), ACM2 (Pleim) boundary layer parameterization (Pleim, 2007), and Rapid Radiative Transfer Model for GCMs radiation scheme (Mlawer et al., 1997). The meteorological initial and boundary conditions are generated from the Final Operational Global Analysis data (ds083.2) of the National Center for Environmental Prediction (NCEP) at a 1.0º × 1.0º and 6-h resolutions. Default profile data is used for chemical initial and boundary conditions. The Meteorology Chemistry Interface Processor (MCIP) version 4.1 is applied to process the meteorological data into a format required by CMAQ. The simulated wind speed, wind direction, temperature and humidity agree well with the observation data from the National Climate Data Center (NCDC), as detailed in the Supplementary Information.

In order to evaluate the high-resolution emission inventory with unit-based industrial sources, we developed a traditional proxy-based emission inventory with the same amount of emissions and compare the simulation results of these two emission inventories. In the proxy-based emission inventory, all sectors are allocated as area sources using spatial proxies such as population, GDP, road map and land use data. The proxies used for each sector is described in detail in Table S2. For the plants not included in the preceding data sources, it is allocated the same as proxy-based emission inventory. In order to separate the influences of horizontal and vertical distributions of emission, we developed another unit-based

inventory with emission heights the same as the proxy-based inventory. In short, we call it hypo unit-based inventory. In the simulation with the unit-based inventory, plume rise is calculated with the built-in algorithm in CMAQ. Meteorological data are used to calculate the plume rise for all point sources. Then, the plume is distributed into the vertical layers that the plume intersects based on the pressure in each layer.

3 Results and discussion

3.1 Air pollutant emissions in Beijing-Tianjin-Hebei region

In the BTH region, the emissions of sulfur dioxide (SO_2), nitrogen oxide (NO_x), PM_{10}, $PM_{2.5}$, black carbon (BC), organic carbon (OC), non-methane volatile organic compounds (NMVOCs) and ammonia (NH_3) are 1417 kt, 2100 kt, 1479 kt, 1106 kt, 213 kt, 289 kt, 2381 kt, and 712 kt in 2014, respectively. **Fig. 2** shows the sectoral emissions for major pollutants in the BTH region by city. **Fig.S2** shows the NMVOCs speciation by sector. The emission estimates are compared with previous studies in **Fig.S3**. **Fig. 3** shows the locations and emissions of power and industrial sources.

Power plants account for 13%, 16%, and 4% of the total SO_2, NO_x, and $PM_{2.5}$ emissions, respectively, and the contributions to NMVOC and NH_3 emissions are negligible (< 1%). For SO_2 and NO_x, power plant is an important emission sources in the BTH region, especially in Tianjin, Shijiazhuang, Tangshan, and Handan.

The emissions from industrial boiler account for 27%, 19%, 8%, 1%, and < 1% of the total SO_2, NO_x, $PM_{2.5}$, NMVOCs, and NH_3 emissions, respectively. As shown in **Fig. 3**, there are many industrial boilers in the BTH region. Industrial boiler is one of the most important emission sources for SO_2 and NO_x.

The emissions from cement contribute 6%, 9%, and 10% of the total SO_2, NO_x, and $PM_{2.5}$ emissions, respectively, and the contributions to NMVOC and NH_3 emissions are negligible (< 1%). Most of cement plants are located in South and East of Hebei.

The emissions from steel represent 8%, 3%, and 22% of the total SO_2, NO_x, and $PM_{2.5}$ emissions, respectively, and the contributions to NMVOC and NH_3 emissions are negligible (< 1%). Tangshan has

the largest number of steel plants in the BTH region, steel accounts for over half of $PM_{2.5}$ emissions in Tangshan.

Besides the aforementioned sectors, 8%, 8%, 13%, 36%, and < 1% of the total SO_2, NO_x, $PM_{2.5}$, NMVOCs, and NH_3 emissions come from other industrial processes (chemistry, coking, nonferrous metal, brick, ceramics, lime, glass, refinery), respectively. Industrial process is the most important emission source for NMVOCs, accounting for nearly half of the emissions in Tianjin and Shijiazhuang.

In total, in the BTH region, industrial sectors (power plant, industrial boiler, cement, steel, and other industrial process) contribute 61%, 55%, 62%, 56%, 58%, 22%, 36% and 0% of the total SO_2, NO_x, PM_{10}, $PM_{2.5}$, BC, OC, NMVOCs, and NH_3 emissions in 2014.

Considering the large contribution of industrial sources to total emissions, the application of unit-based method results in remarkable changes in the spatial distribution of air pollutant emissions. The emission rates of $PM_{2.5}$, NO_x and SO_2 of the proxy-based and unit-based inventories and their differences are shown in **Fig. 4**. In the unit-based emission inventory, the emission is lower than that in the proxy-based emission inventory in the urban centers of BTH region. Instead, a large amount of the emission is concentrated in certain points in suburban areas, where large plants are located.

3.2 Evaluation of the unit-based emission inventory

In order to study the accuracy of the unit-based inventory, the simulation results of SO_2, NO_2, ozone and $PM_{2.5}$ with the unit-based inventory are compared with the observational data from China National Environmental Monitoring Centre. The observations are available for eighty sites located in 13 cities in the BTH region, including 70 sites in urban area and 10 sites in suburban area. The accurate location of urban and suburban sites in Beijing is shown in Fig.S5-S6. The analysis of the results is shown in **Table 1**. We use normalized mean bias (NMB), normalized mean error (NME), mean fractional bias (MFB) and mean fractional error (MFE) (EPA, 2007) to quantitatively evaluate the model performance.

SO_2 and NO_2 are precursors of $PM_{2.5}$, so we first compare the simulation results of gaseous pollutants with observations. For NO_2, the results with proxy-based inventory overestimates the observations by 22% while results with unit-based inventory overestimates by 9% in January. Similarly, in July, the

simulated NO_2 concentrations show overestimation in simulations with both inventories but the overestimation is less with unit-based inventory. The simulation results of SO_2 is similar to those of NO_2. However, the overestimation is higher with both inventories and the differences between the concentrations with two inventories are larger. The overestimation of SO_2 concentrations may be due to the lack of several SO_2 reaction mechanisms in CMAQ, such as heterogeneous reactions of SO_2 on the surface of dust particles (Fu et al., 2016), the oxidation of SO_2 by NOx in aerosol liquid water (Cheng et al., 2016;Wang et al., 2016a), the effects of SO_2 and NH_3 on secondary organic aerosol formation (Chu et al., 2016), etc. The biased spatial distribution of SO_2 emissions from residential combustion may also contribute to the overestimation. A large fraction of residential combustion takes place in the rural areas. In this work, however, the emission of residential combustion is allocated by GDP and population, which leads to an overestimation of SO_2 emission in urban area and hence an overestimation of SO_2 concentration.

For ozone, the simulation results in January with proxy-based inventory underestimate the observations by 21% while the results with unit-based inventory underestimate by only 5%. The simulation results in July follows the same trend. China is experiencing more and more severe ozone pollution these years (Li et al., 2019), which usually occurs in summer. Therefore, we analyse two extra indices of ozone, 1-hour-peak ozone and daily maximum 8-h averaged (MDA8) ozone concentration in July, which are shown in **Table 2**. The results of 1-hour-peak ozone and MDA8 ozone concentration is similar to that of monthly average ozone concentration. The concentration with the unit-based inventory is slightly higher than that with proxy-based inventory and closer to the observation. The reason for the changes in ozone concentrations will be discussed later.

The simulated $PM_{2.5}$ concentrations with unit-based inventory are lower than that with proxy-based inventory in both winter and summer. In January, the simulated $PM_{2.5}$ concentrations with proxy-based inventory overestimates the observed values by 25% while the overestimation is 7% with unit-based inventory. In July, the simulated $PM_{2.5}$ concentrations with both inventories are 17% and 30% lower than the observations, respectively. An overall underestimation is as expected because the default CMAQ model underestimates the concentrations of secondary organic aerosol (Zhao et al., 2016) significantly

and the fugitive dust emission is not included in the emission inventory. According to Boylan and Russell (2006), the simulation results of PM is acceptable when Mean Fractional Bias (MFB) is less than or equal to ±60% and Mean Fractional Bias (MFE) is less than 75% and a model performance goal is met when MFB is less than ±30% and MFE is less than 50%. The statistical indices of the simulation results of $PM_{2.5}$ with both inventories and both months are within the performance goal value, which means that the simulation results are relatively accurate.

Fig. 5 further shows the spatial distribution of SO_2, NO_2, ozone, 1-hour-peak ozone, MDA8 ozone and $PM_{2.5}$ concentrations with the proxy-based inventory, the differences between the other two simulations and proxy-based inventory. For SO_2, NO_2 and $PM_{2.5}$, the concentrations in the urban area is generally higher with proxy-based inventory than that with unit-based inventory, especially in winter. In January, large difference of concentrations of simulations with two inventories are found in urban Tianjin, Tangshan, Baoding and Shijiazhuang, where a large amount of industrial emissions are allocated in the proxy-based inventory due to large population density. The simulation of July follows the same pattern but the concentrations and the difference between the concentrations with two inventories are lower than those of January. In some areas where many factories are located, such like the northern part of Xingtai city, the concentration with unit-based inventory is higher because of the high emission intensity. There are two reasons for the difference between results with two inventories. The first one is the spatial distribution. With detailed information of industrial sectors, more emissions are allocated to certain locations in suburban/rural areas in the unit-based emission inventory. From “Diff1” (hypo unit-based minus proxy-based), we can see that the improved horizontal distribution of the unit-based emission inventory significantly decreases the $PM_{2.5}$, SO_2, and NO_2 concentrations in most urban centers, and significantly increases the concentrations in a large fraction of suburban and rural areas, especially the areas where large industrial plants are located in. The other reason is vertical distribution. Plume rise is calculated in the simulation with the unit-based inventory, which causes the difference of emissions in vertical layers. The higher the pollutants are emitted, the lower the ground concentration becomes. From the differences between Diff1 and Diff2 we can see that the plume rise leads to lower concentrations over the whole region.

For ozone, the difference of concentration is evident but opposite to that of $PM_{2.5}$. This is because that urban centers of Beijing/Tianjin are located in the VOC-control chemical regime (Liu et al., 2010). The emissions of NO_x in surface layer are less in the unit-based inventory than in the proxy-based inventory, which leads to higher ozone concentration in urban area.

The spatial distribution of concentrations of these pollutants are significantly heterogeneous. The NME and MFE of most pollutants in two months are lower with unit-based inventory than with proxy-based inventory, which means the spatial distribution with unit-based inventory agrees more with the observation than that of unit-based inventory. For SO_2, NO_2 and $PM_{2.5}$, peak concentrations usually occur in the urban center while it's the opposite for ozone. We apply the metric of "concentration gradient", which is defined as the ratios of urban monthly mean concentrations to suburban concentrations, to quantitatively characterize the heterogeneous spatial distributions. We calculate the concentration gradients for Beijing and Tianjin (**Fig. 6**), since there are both urban and suburb observational sites in these two cities. The concentration gradient of NO_2 and SO_2 between urban and suburban areas is closer to the observations in the simulation with unit-based inventory than that with proxy-based inventory (**Fig. 6**). The simulated O_3 concentration gradients with unit-based, proxy-based inventories and the observation are 0.7, 0.5 and 0.9 in January and 0.9, 0.8 and 1.1 in July. As for 1h-peak and MDA8 ozone in July, the simulated results with unit-based inventory is also closer to the observation. As stated previously, this is explained by the VOC-limited photochemical regime and lower NO_x emissions in the unit-based inventory over the urban areas. As for $PM_{2.5}$, the concentration gradients for simulations with unit-based, proxy-based inventories and observations in Beijing are 1.6, 2.1 and 1.5 in January and 1.3, 1.5 and 1.3 in July. The results imply that the unit-based emission inventory better reproduces the distributions of pollutant emissions between the urban and suburban areas.

To further elucidate the reasons for the difference between the $PM_{2.5}$ concentrations with two emission inventories, we examine the simulation results of different chemical components, including sulfate (SO_4^{2-}), nitrate (NO_3^-), ammonium (NH_4^+), element carbon (EC) and organic carbon (OC), as shown in **Fig. 7** and **Table 2**. The concentrations of EC and OC in the simulation with unit-based inventory are generally lower than that with proxy-based inventory in both January and July, especially in urban

Beijing, Baoding and Shijiazhuang. This pattern is similar to that of $PM_{2.5}$. In some cities such as Xingtai, the concentrations of EC and OC in the simulation with unit-based inventory are slightly higher than that with proxy-based inventory.

The results of secondary inorganic aerosols are quite different. From **Fig. 7** and **Table 2** we can see that the sulfate concentrations is lower in most areas in the simulation with unit-based inventory as compared to that with proxy-based inventory, which is because that the sensitivity of sulfate concentrations to SO_2 concentration is positive during all months (Zhao et al., 2017b). The differences of the concentration of sulfate is similar to that of SO_2, which is shown in **Fig. 5**. The difference of ammonium concentration is relatively small compared with other components. As for nitrate, concentration of nitrate in the simulation with unit-based inventory is much higher than that with proxy-based inventory in winter while the differences between the results with two inventories vary with location in summer. Sulfate concentrations in the unit-based approach are much lower than the proxy-based approach whereas ammonium is almost constant as shown in **Fig. 7**. In this case, more HNO_3 is converted to NO_3^- with excess NH_4^+ whereas these processes depend on abundance of HNO_3 or NH_3. Taking all chemical components into account, the primary components account for most of the differences in $PM_{2.5}$ concentrations between the simulations with two inventories. In contrast, however, the complex responses of various secondary components often counteract each other (especially in January), leading to an overall smaller contribution of secondary components to the $PM_{2.5}$ concentration differences.

4 Conclusion

In this study, we developed a high-resolution emission inventory of major pollutants for BTH region for year 2014 with unit-based emissions from industrial sectors. The emissions of SO_2, NO_x, PM_{10}, $PM_{2.5}$, BC, OC and NMVOCs from industrial sectors are 869 kt, 1164 kt, 910 kt, 622 kt, 71 kt, 63 kt and 1390 kt respectively, accounting for 61%, 55%, 62%, 56%, 58%, 22% and 36% of the total emissions.

The emissions in unit-based emission inventory are lower than that in the proxy-based emission inventory in most urban centers of the BTH region because of the concentrated emissions in point sources. The

application of the unit-based emission inventory improves model-observation agreement for most pollutants. The accurate location of point sources leads to lower concentration of primary pollutants in urban area and higher in suburban area. The plume rise accounts for the lower concentration of the whole region. For SO_2, NO_2 and $PM_{2.5}$, the concentrations in the urban area decrease significantly and become closer to the observations mostly due to the decrease of urban emissions. For ozone, the concentrations in the urban area increase slightly and also show better agreement with observations mainly due to the more reasonable allocation of NO_x emissions. The improvement is particularly significant for the urban-suburban concentration gradients. For $PM_{2.5}$, the concentration gradients for the simulations with unit-based, proxy-based inventories and observations in Beijing are 1.6, 2.1 and 1.5 in January and 1.3, 1.5 and 1.3 in July. For ozone, the corresponding values are 0.7, 0.5 and 0.9 in January and 0.9, 0.8 and 1.1 in July, implying that the unit-based emission inventory better reproduces the distributions of pollutant emissions between the urban and suburban areas.

The unit-based industrial emission inventory enables more accurate source apportionment and more reliable research on air pollution formation mechanism, and therefore contributes to the development of more precisely targeted control policies. To further improve the emission inventory, it is necessary to improve the spatial allocation of emissions from non-industrial sectors, such as the residential and commercial sectors. Our previous study provides an example to develop a village-based residential emission inventory in rural Beijing (Cai et al., 2018). Such studies on high-resolution emission inventories, for both industrial and nonindustrial sources, are highly needed and should be extended to other provinces and/or regions as well.

Acknowledgements

This research has been supported by the National Natural Science Foundation of China (21625701), Strategic Priority Research Program of Chinese Academy of Sciences (XDA20040502), the Ministry of Environmental Protection of China (DQGG0301) and Beijing Municipal Commission of Science and

Technology (D171100001517001). The simulations were completed on the “Explorer 100” cluster system of Tsinghua National Laboratory for Information Science and Technology.

References

Beijing Municipal Bureau of Statistics: Beijing Statistical Yearbook 2014, China Statistics Press, Beijing, 2015.

Boylan, J. W., and Russell, A. G.: PM and light extinction model performance metrics, goals, and criteria for three-dimensional air quality models, Atmos Environ, 40, 4946-4959, 10.1016/j.atmonsenv.2005.09.087, 2006.

Briggs, G. A.: Plume Rise Predictions, in: Lectures on Air Pollution and Environmental Impact Analyses, edited by: Haugen, D. A., American Meteorological Society, Boston, MA, 59-111, 1982.

Cai, S., Li, Q., Wang, S., Chen, J., Ding, D., Zhao, B., Yang, D., and Hao, J.: Pollutant emissions from residential combustion and reduction strategies estimated via a village-based emission inventory in Beijing, Environmental pollution (Barking, Essex : 1987), 238, 230-237, 10.1016/j.envpol.2018.03.036, 2018.

Chen, L., Sun, Y., Wu, X., Zhang, Y., Zheng, C., Gao, X., and Cen, K.: Unit-based emission inventory and uncertainty assessment of coal-fired power plants, Atmos Environ, 99, 527-535, 10.1016/j.atmosenv.2014.10.023, 2014.

Chen, W., Hong, J., and Xu, C.: Pollutants generated by cement production in China, their impacts, and the potential for environmental improvement, Journal of Cleaner Production, 103, 61-69, 10.1016/j.jclepro.2014.04.048, 2015.

Cheng, Y., Zheng, G., Wei, C., Mu, Q., Zheng, B., Wang, Z., Gao, M., Zhang, Q., He, K., Carmichael, G., Poschl, U., and Su, H.: Reactive nitrogen chemistry in aerosol water as a source of sulfate during haze events in China, Science Advances, 2, 10.1126/sciadv.1601530, 2016.

China Electricity Council: Compilation of power industry statistics 2014, China Electricity Council, Beijing, 2015a.

China Electricity Council: Annual Development Report for China Electric Power Industry 2014, China Statistics Press, Beijing, 2015b.

Chinese State Council: Atmospheric Pollution Prevention and Control Action Plan, Chinese State Council, Beijing, 2013.

Chu, B., Zhang, X., Liu, Y., He, H., Sun, Y., Jiang, J., Li, J., and Hao, J.: Synergetic formation of secondary inorganic and organic aerosol: effect of SO₂ and NH₃ on particle formation and growth, Atmos Chem Phys, 16, 14219-14230, 10.5194/acp-16-14219-2016, 2016.

EPA, U.: Guidance on the Use of Models and Other Analyses for Demonstrating Attainment of Air Quality Goals for Ozone, PM2.5, and Regional Haze, 2007.

CMAQv5.0.2 (Version 5.0.2), 2014.

Fu, X., Wang, S. X., Zhao, B., Xing, J., Cheng, Z., Liu, H., and Hao, J. M.: Emission inventory of primary

pollutants and chemical speciation in 2010 for the Yangtze River Delta region, China, Atmos Environ, 70, 39-50, 10.1016/j.atmosenv.2012.12.034, 2013.

Fu, X., Wang, S., Chang, X., Cai, S., Xing, J., and Hao, J.: Modeling analysis of secondary inorganic aerosols over China: pollution characteristics, and meteorological and dust impacts, Sci Rep, 6, 35992, 10.1038/srep35992, 2016.

Geng, G., Zhang, Q., Martin, R. V., Lin, J., Huo, H., Zheng, B., Wang, S., and He, K.: Impact of spatial proxies on the representation of bottom-up emission inventories: A satellite-based analysis, Atmos Chem Phys, 17, 4131-4145, 10.5194/acp-17-4131-2017, 2017.

Hebei Municipal Bureau of Statistics: Hebei Statistical Yearbook 2014, China Statistics Press, Hebei, 2015.

Kain, J. S.: The Kain-Fritsch convective parameterization: An update, Journal of Applied Meteorology, 43, 170-181, 10.1175/1520-0450(2004)043<0170:tkcpau>2.0.co;2, 2004.

Lei, Y., Zhang, Q., Nielsen, C., and He, K.: An inventory of primary air pollutants and CO2 emissions from cement production in China, 1990-2020, Atmos Environ, 45, 147-154, 10.1016/j.atmosenv.2010.09.034, 2011.

Li, K., Jacob, D. J., Liao, H., Shen, L., Zhang, Q., and Bates, K. H.: Anthropogenic drivers of 2013-2017 trends in summer surface ozone in China, Proceedings of the National Academy of Sciences of the United States of America, 116, 422-427, 10.1073/pnas.1812168116, 2019.

Li, M., Zhang, Q., Kurokawa, J., Woo, J. H., He, K. B., Lu, Z. F., Ohara, T., Song, Y., Streets, D. G., Carmichael, G. R., Cheng, Y. F., Hong, C. P., Huo, H., Jiang, X. J., Kang, S. C., Liu, F., Su, H., and Zheng, B.: MIX: a mosaic Asian anthropogenic emission inventory under the international collaboration framework of the MICS-Asia and HTAP, Atmos Chem Phys, 17, 935-963, 10.5194/acp-17-935-2017, 2017.

Liu, F., Zhang, Q., Tong, D., Zheng, B., Li, M., Huo, H., and He, K. B.: High-resolution inventory of technologies, activities, and emissions of coal-fired power plants in China from 1990 to 2010, Atmos Chem Phys, 15, 13299-13317, 2015.

Liu, X. H., Zhang, Y., Xing, J., Zhang, Q. A., Wang, K., Streets, D. G., Jang, C., Wang, W. X., and Hao, J. M.: Understanding of regional air pollution over China using CMAQ, part II. Process analysis and sensitivity of ozone and particulate matter to precursor emissions, Atmos Environ, 44, 3719-3727, 10.1016/j.atmosenv.2010.03.036, 2010.

Ministry of Environmental Protection of China: Emission standard of air pollutants for industrial kiln and furnace, Ministry of Environmental Protection of China (MEP), Beijing, 1997.

Ministry of Environmental Protection of China: Emission standard of air pollutants for cement industry, Ministry of Environmental Protection of China (MEP), Beijing, 2013.

Mlawer, E. J., Taubman, S. J., Brown, P. D., Iacono, M. J., and Clough, S. A.: Radiative transfer for inhomogeneous atmospheres: RRTM, a validated correlated-k model for the longwave, J Geophys Res-Atmos, 102, 16663-16682, 10.1029/97jd00237, 1997.

Morrison, H., Curry, J. A., and Khvorostyanov, V. I.: A new double-moment microphysics parameterization for application in cloud and climate models. Part I: Description, Journal of the Atmospheric Sciences, 62, 1665-1677, 10.1175/jas3446.1, 2005.

National Bureau of Statistics (NBS): Report of the first national census of pollution sources, China Statistics Press, Beijing, 2010.
National Bureau of Statistics (NBS): China Steel Yearbook 2011, China Statistics Press, Beijing, 2012.
National Bureau of Statistics (NBS): China Urban Construction Statistical Yearbook 2014, China Statistics Press, Beijing, 2015a.
National Bureau of Statistics (NBS): China Agriculture Yearbook 2014, China Statistics Press, Beijing, 2015b.
National Bureau of Statistics (NBS): China Chemical Industry yearbook 2014, China Statistics Press, Beijing, 2015c.
National Bureau of Statistics (NBS): China Electric Power Yearbook 2014, China Statistics Press, Beijing, 2015d.
National Bureau of Statistics (NBS): China Energy Statistical Yearbook 2014, China Statistics Press, Beijing, 2015e.
National Bureau of Statistics (NBS): China Environmental Statistical Yearbook 2014, China Statistics Press, Beijing, 2015f.
National Bureau of Statistics (NBS): China Industrial Economic Statistical Yearbook 2014, China Statistics Press, Beijing, 2015g.
National Bureau of Statistics (NBS): China Regional Economic Statistical Yearbook 2014, China Statistics Press, Beijing, 2015h.
National Bureau of Statistics (NBS): China Rural Statistical Yearbook 2014, China Statistics Press, Beijing, 2015i.
National Bureau of Statistics (NBS): China Statistical Yearbook 2014, China Statistics Press, Beijing, 2015j.
Oda, T., and Maksyutov, S.: A very high-resolution (1 km×1 km) global fossil fuel CO₂ emission inventory derived using a point source database and satellite observations of nighttime lights, Atmos Chem Phys, 11, 543-556, 10.5194/acp-11-543-2011, 2011.
Ohara, T., Akimoto, H., Kurokawa, J., Horii, N., Yamaji, K., Yan, X., and Hayasaka, T.: An Asian emission inventory of anthropogenic emission sources for the period 1980-2020, Atmos Chem Phys, 7, 4419-4444, 10.5194/acp-7-4419-2007, 2007.
Pleim, J. E.: A simple, efficient solution of flux-profile relationships in the atmospheric surface layer, Journal of Applied Meteorology and Climatology, 45, 341-347, 10.1175/jam2339.1, 2006.
Pleim, J. E.: A Combined Local and Nonlocal Closure Model for the Atmospheric Boundary Layer. Part II: Application and Evaluation in a Mesoscale Meteorological Model, Journal of Applied Meteorology and Climatology, 46, 1396-1409, 10.1175/jam2534.1, 2007.
Qi, J., Zheng, B., Li, M., Yu, F., Chen, C., Liu, F., Zhou, X., Yuan, J., Zhang, Q., and He, K.: A high-resolution air pollutants emission inventory in 2013 for the Beijing-Tianjin-Hebei region, China, Atmos Environ, 170, 156-168, 10.1016/j.atmosenv.2017.09.039, 2017.
Sarwar, G., Appel, K. W., Carlton, A. G., Mathur, R., Schere, K., Zhang, R., and Majeed, M. A.: Impact of a new condensed toluene mechanism on air quality model predictions in the US, Geoscientific Model Development, 4, 183-193, 10.5194/gmd-4-183-2011, 2011.

Skamarock, W. C., Dudhia, J. B. K. J., Gill, D. O., Barker, D., Wang, W., and Powers, J. G.: A Description of the Advanced Research WRF Version 3, NCAR Technical Note NCAR/TN-475+STR, 10.5065/D68S4MVH, 2008.

Stohl, A., Aamaas, B., Amann, M., Baker, L. H., Bellouin, N., Berntsen, T. K., Boucher, O., Cherian, R., Collins, W., Daskalakis, N., Dusinska, M., Eckhardt, S., Fuglestvedt, J. S., Harju, M., Heyes, C., Hodnebrog, O., Hao, J., Im, U., Kanakidou, M., Klimont, Z., Kupiainen, K., Law, K. S., Lund, M. T., Maas, R., MacIntosh, C. R., Myhre, G., Myriokefalitakis, S., Olivie, D., Quaas, J., Quennehen, B., Raut, J. C., Rumbold, S. T., Samset, B. H., Schulz, M., Seland, O., Shine, K. P., Skeie, R. B., Wang, S., Yttri, K. E., and Zhu, T.: Evaluating the climate and air quality impacts of short-lived pollutants, Atmos Chem Phys, 15, 10529-10566, 10.5194/acp-15-10529-2015, 2015.

Streets, D. G., Bond, T. C., Carmichael, G. R., Fernandes, S. D., Fu, Q., He, D., Klimont, Z., Nelson, S. M., Tsai, N. Y., Wang, M. Q., Woo, J. H., and Yarber, K. F.: An inventory of gaseous and primary aerosol emissions in Asia in the year 2000, J Geophys Res-Atmos, 108, 10.1029/2002jd003093, 2003.

Tianjin Municipal Bureau of Statistics: Tianjin Statistical Yearbook 2014, China Statistics Press, Tianjin, 2015.

Wang, G., Zhang, R., Gomez, M. E., Yang, L., Levy Zamora, M., Hu, M., Lin, Y., Peng, J., Guo, S., Meng, J., Li, J., Cheng, C., Hu, T., Ren, Y., Wang, Y., Gao, J., Cao, J., An, Z., Zhou, W., Li, G., Wang, J., Tian, P., Marrero-Ortiz, W., Secrest, J., Du, Z., Zheng, J., Shang, D., Zeng, L., Shao, M., Wang, W., Huang, Y., Wang, Y., Zhu, Y., Li, Y., Hu, J., Pan, B., Cai, L., Cheng, Y., Ji, Y., Zhang, F., Rosenfeld, D., Liss, P. S., Duce, R. A., Kolb, C. E., and Molina, M. J.: Persistent sulfate formation from London Fog to Chinese haze, Proc Natl Acad Sci U S A, 10.1073/pnas.1616540113, 2016a.

Wang, K., Tian, H., Hua, S., Zhu, C., Gao, J., Xue, Y., Hao, J., Wang, Y., and Zhou, J.: A comprehensive emission inventory of multiple air pollutants from iron and steel industry in China: Temporal trends and spatial variation characteristics, Sci Total Environ, 559, 7-14, 10.1016/j.scitotenv.2016.03.125, 2016b.

Wang, S. X., Zhao, B., Cai, S. Y., Klimont, Z., Nielsen, C. P., Morikawa, T., Woo, J. H., Kim, Y., Fu, X., Xu, J. Y., Hao, J. M., and He, K. B.: Emission trends and mitigation options for air pollutants in East Asia, Atmos Chem Phys, 14, 6571-6603, 10.5194/acp-14-6571-2014, 2014.

Wu, W., Zhao, B., Wang, S., and Hao, J.: Ozone and secondary organic aerosol formation potential from anthropogenic volatile organic compounds emissions in China, J Environ Sci (China), 53, 224-237, 10.1016/j.jes.2016.03.025, 2017.

Wu, X., Zhao, L., Zhang, Y., Zheng, C., Gao, X., and Cen, K.: Primary Air Pollutant Emissions and Future Prediction of Iron and Steel Industry in China, Aerosol and Air Quality Research, 15, 1422-1432, 10.4209/aaqr.2015.01.0029, 2015.

Xiu, A. J., and Pleim, J. E.: Development of a land surface model. Part I: Application in a mesoscale meteorological model, Journal of Applied Meteorology, 40, 192-209, 10.1175/1520-0450(2001)040<0192:doalsm>2.0.co;2, 2001.

Xue, Y., Tian, H., Yan, J., Zhou, Z., Wang, J., Nie, L., Pan, T., Zhou, J., Hua, S., Wang, Y., and Wu, X.: Temporal trends and spatial variation characteristics of primary air pollutants emissions from coal-fired industrial boilers in Beijing, China, Environ Pollut, 213, 717-726, 10.1016/j.envpol.2016.03.047, 2016.

Zhao, B., Wang, S., Dong, X., Wang, J., Duan, L., Fu, X., Hao, J., and Fu, J.: Environmental effects of

the recent emission changes in China: implications for particulate matter pollution and soil acidification, Environmental Research Letters, 8, 024031, 10.1088/1748-9326/8/2/024031, 2013a.

Zhao, B., Wang, S. X., Wang, J. D., Fu, J. S., Liu, T. H., Xu, J. Y., Fu, X., and Hao, J. M.: Impact of national NOx and SO2 control policies on particulate matter pollution in China, Atmos Environ, 77, 453-463, 10.1016/j.atmosenv.2013.05.012, 2013b.

Zhao, B., Wang, S., Donahue, N. M., Jathar, S. H., Huang, X., Wu, W., Hao, J., and Robinson, A. L.: Quantifying the effect of organic aerosol aging and intermediate-volatility emissions on regional-scale aerosol pollution in China, Sci Rep, 6, 28815, 10.1038/srep28815, 2016.

Zhao, B., Wu, W., Wang, S., Xing, J., Chang, X., Liou, K.-N., Jiang, J. H., Gu, Y., Jang, C., Fu, J. S., Zhu, Y., Wang, J., Lin, Y., and Hao, J.: A modeling study of the nonlinear response of fine particles to air pollutant emissions in the Beijing-Tianjin-Hebei region, Atmos Chem Phys, 17, 12031-12050, 10.5194/acp-17-12031-2017, 2017a.

Zhao, B., Wu, W. J., Wang, S. X., Xing, J., Chang, X., Liou, K. N., Jiang, J. H., Gu, Y., Jang, C., Fu, J. S., Zhu, Y., Wang, J. D., Lin, Y., and Hao, J. M.: A modeling study of the nonlinear response of fine particles to air pollutant emissions in the Beijing-Tianjin-Hebei region, Atmos Chem Phys, 17, 12031-12050, 10.5194/acp-17-12031-2017, 2017b.

Zhao, Y., Wang, S. X., Duan, L., Lei, Y., Cao, P. F., and Hao, J. M.: Primary air pollutant emissions of coal-fired power plants in China: Current status and future prediction, Atmos Environ, 42, 8442-8452, 10.1016/j.atmosenv.2008.08.021, 2008.

Zhao, Y., Mao, P., Zhou, Y. D., Yang, Y., Zhang, J., Wang, S. K., Dong, Y. P., Xie, F. J., Yu, Y. Y., and Li, W. Q.: Improved provincial emission inventory and speciation profiles of anthropogenic non-methane volatile organic compounds: a case study for Jiangsu, China, Atmos Chem Phys, 17, 7733-7756, 10.5194/acp-17-7733-2017, 2017c.

Zheng, B., Zhang, Q., Tong, D., Chen, C., Hong, C., Li, M., Geng, G., Lei, Y., Huo, H., and He, K.: Resolution dependence of uncertainties in gridded emission inventories: a case study in Hebei, China, Atmos Chem Phys, 17, 921-933, 10.5194/acp-17-921-2017, 2017.

Zhou, Y., and Gurney, K. R.: Spatial relationships of sector-specific fossil fuel CO2emissions in the United States, Global Biogeochemical Cycles, 25, n/a-n/a, 10.1029/2010gb003822, 2011.

Figures

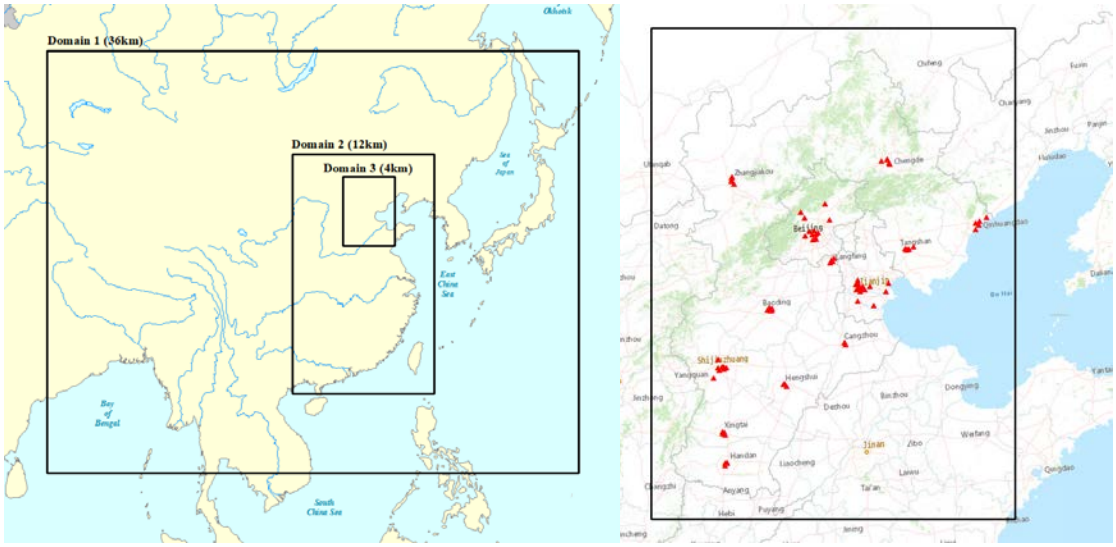

Fig. 1 The three-nested CMAQ domain (left) and the observational sites in Beijing-Tianjin-Hebei region (right)

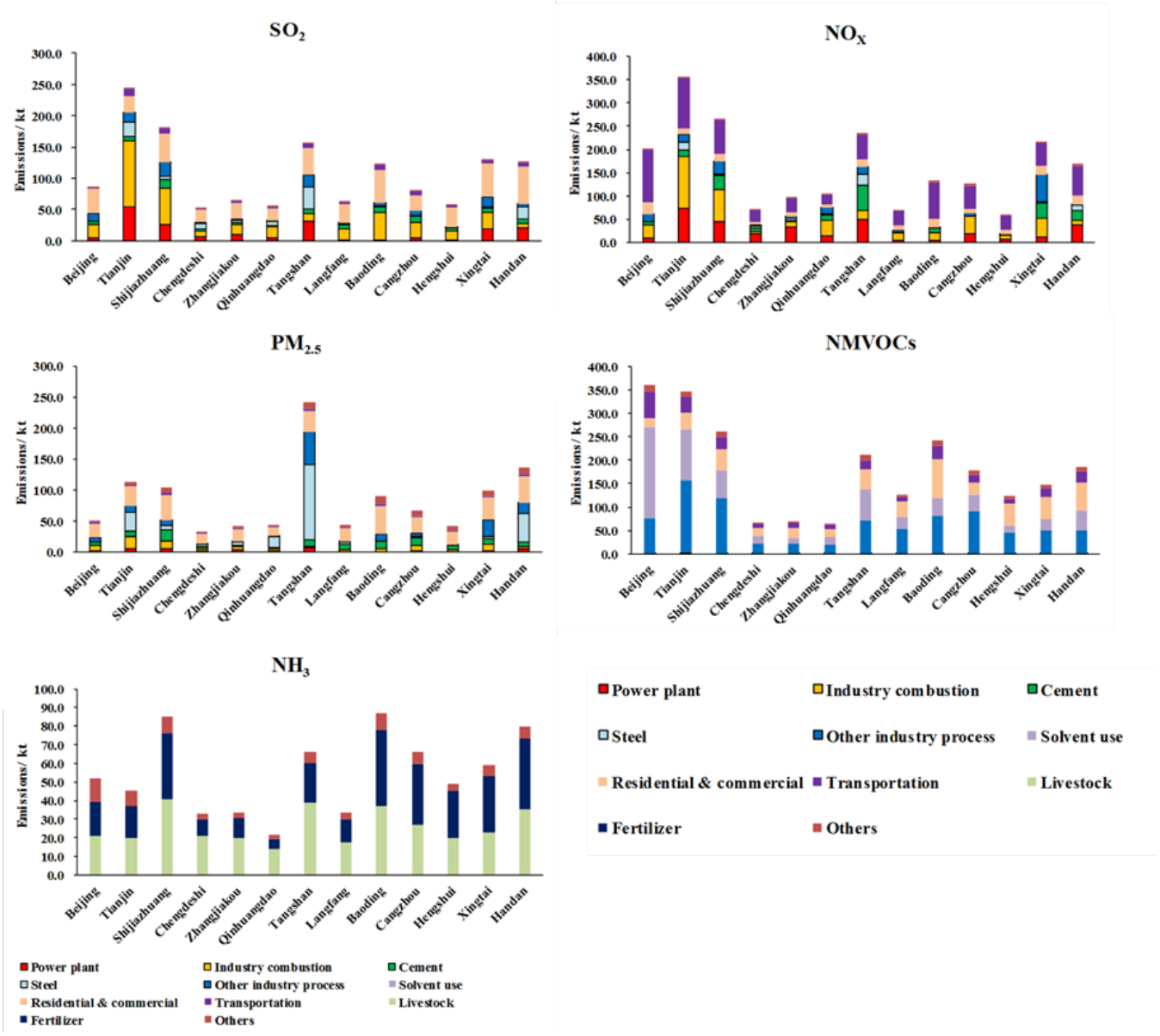

Fig. 2 Sectoral contributions to emissions in BTH region in 2014

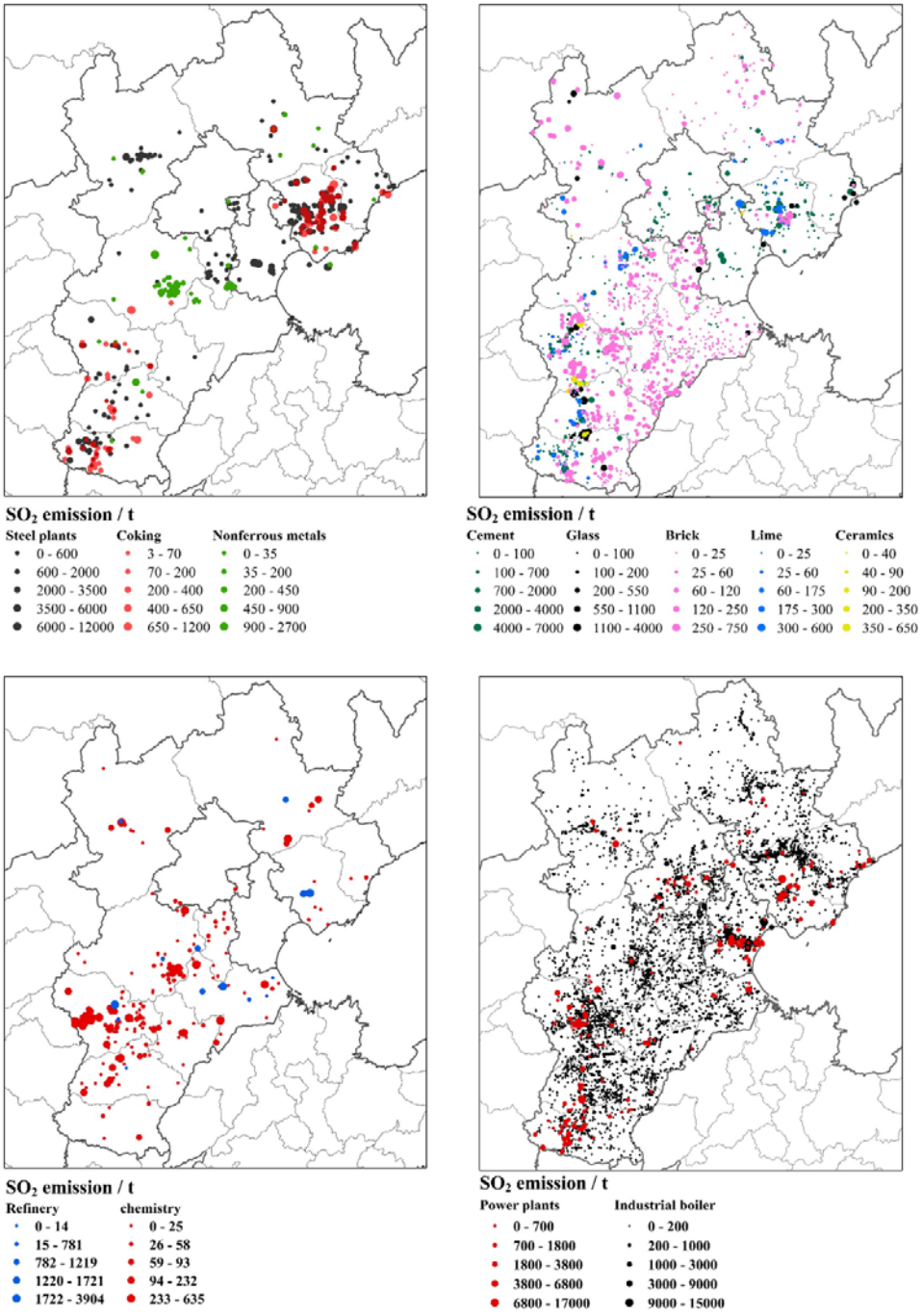

Fig. 3 Locations and emissions of industrial sources in the BTH region. The industrial plants are divided into four groups to display more clearly.

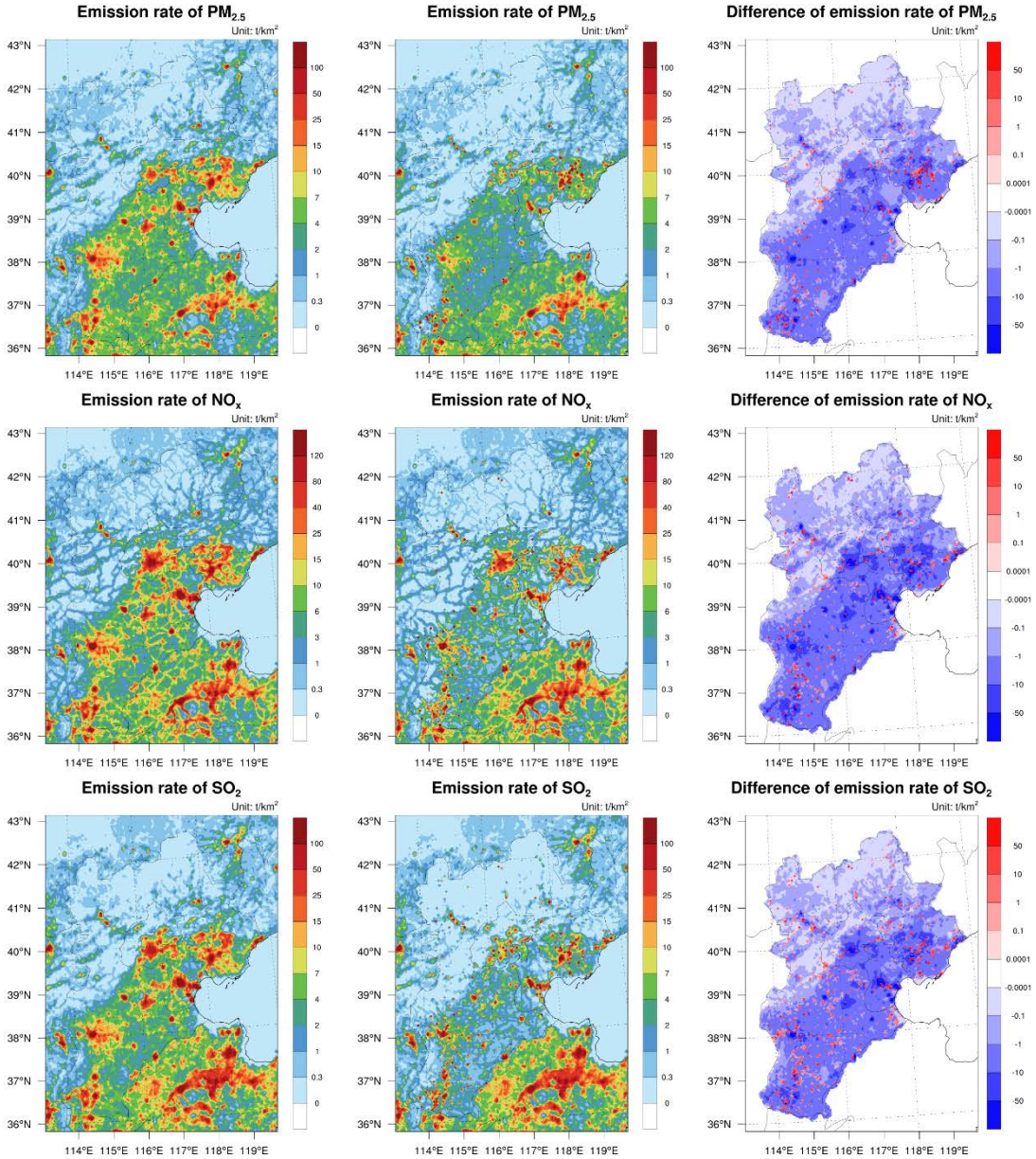

Fig. 4 Emission rate of $PM_{2.5}$, NO_x and SO_2 emissions of the proxy-based (left column) and unit-based (middle column) inventories and their differences (unit-based minus proxy-based, right column). Note that the emissions are the same in provinces other than Beijing, Tianjin, and Hebei.

5

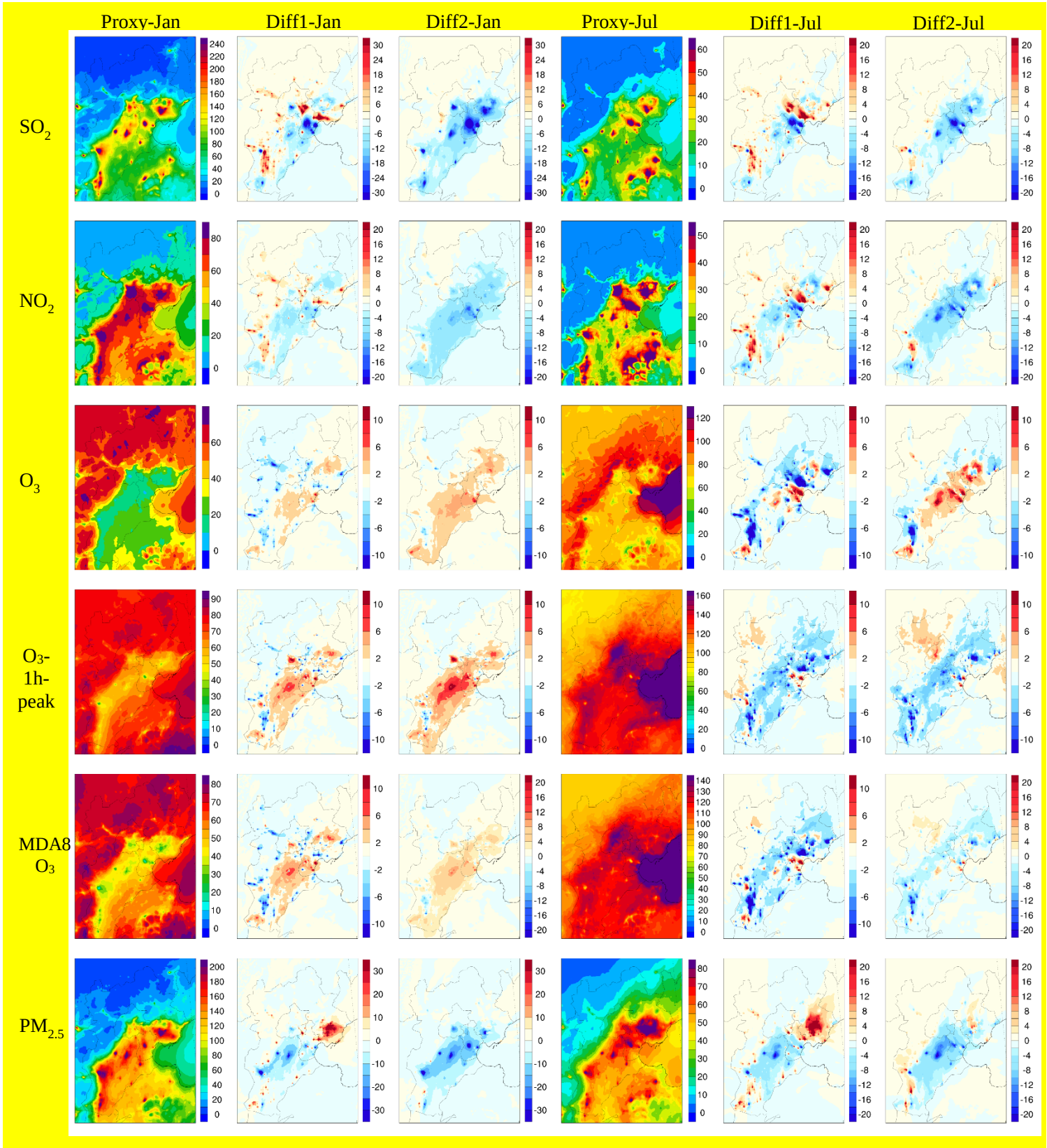

Fig. 5 Spatial distribution of the monthly (January and July) mean concentrations of SO_2, NO_2, ozone, 1h-peak ozone, MDA8 ozone and $PM_{2.5}$ with the proxy-based inventory, and the differences between the other two simulations and proxy-based inventory (Diff1: hypo unit-based minus proxy-based; Diff2: unit-based minus proxy-based). The units are $\mu g/m^3$ for all panels.

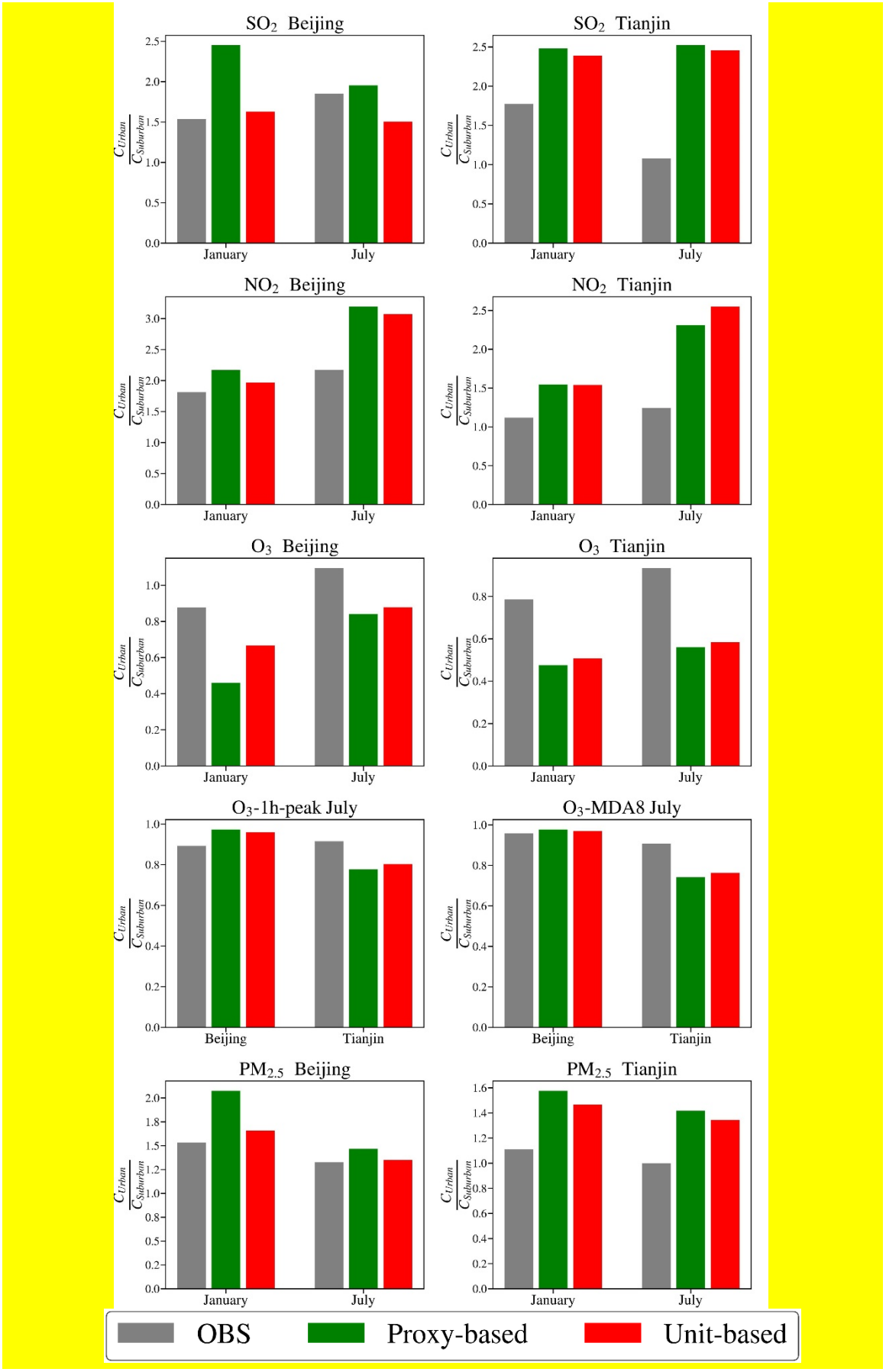

Fig. 6 Observed and simulated concentration gradients of NO_2, $PM_{2.5}$, ozone and SO_2 with the proxy-based and unit-based inventories in Beijing (left) and Tianjin (right)

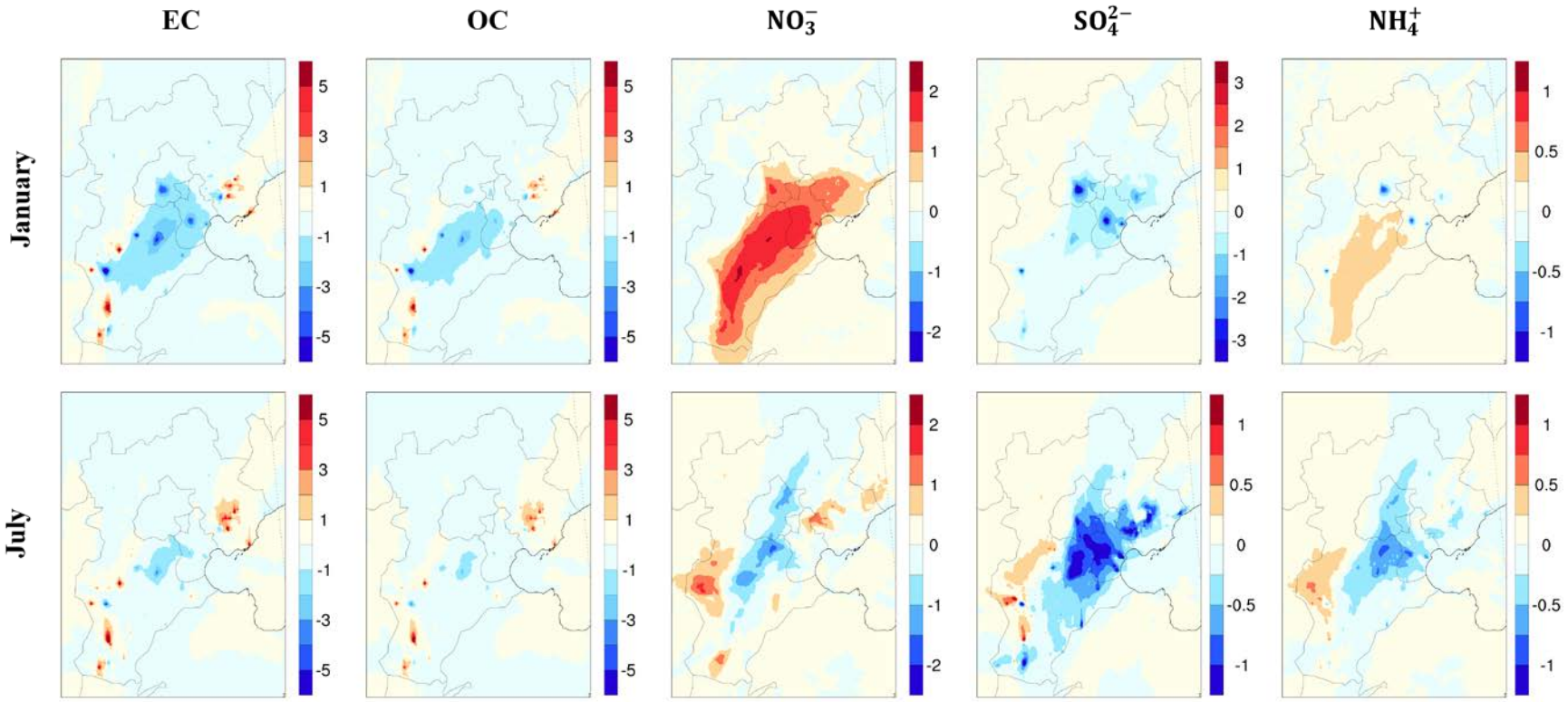

Fig. 7 The differences (unit: μg/m^3) in the simulation results of the components of $PM_{2.5}$ between the results with two inventories (unit-based minus proxy-based).

Table 1. The statistics for model performance of $PM_{2.5}$, NO_2, SO_2, 1-hour-peak ozone and daily maximum 8-h averaged (MDA8) ozone in January and July of 2014 with proxy-based and unit-based inventories

Month	Species	Emission	SIM ($\mu g/m^3$)	OBS ($\mu g/m^3$)	NME	NMB	MFB	MFE
Jan	SO_2	Proxy-based	251.9	112.3	131%	124%	51%	57%
		Unit-based	207.8		93%	85%	35%	42%
	NO_2	Proxy-based	88.0	72.0	30%	22%	14%	19%
		Unit-based	77.9		23%	8%	5%	16%
	O_3	Proxy-based	16.8	21.4	36%	-21%	-19%	27%
		Unit-based	20.2		33%	-6%	-6%	22%
	$PM_{2.5}$	Proxy-based	176.3	141.1	39%	25%	12%	22%
		Unit-based	151.5		31%	7%	2%	20%
Jul	SO_2	Proxy-based	58.4	26.4	140%	121%	54%	63%
		Unit-based	42.7		86%	62%	34%	47%
	NO_2	Proxy-based	61.5	35.9	80%	72%	33%	40%
		Unit-based	52.1		62%	45%	20%	34%
	O_3	Proxy-based	64.0	66.8	96%	-4%	-26%	26%
		Unit-based	69.0		90%	3%	-21%	22%
	$PM_{2.5}$	Proxy-based	71.2	85.5	26%	-17%	-12%	19%
		Unit-based	60.1		34%	-30%	-21%	25%
Two-month average	SO_2	Proxy-based	155.2	69.4	133%	124%	53%	60%
		Unit-based	125.2		92%	81%	35%	45%
	NO_2	Proxy-based	74.7	53.9	47%	39%	23%	30%
		Unit-based	65.0		36%	21%	13%	25%
	O_3	Proxy-based	40.4	44.1	82%	-8%	-22%	27%
		Unit-based	44.6		76%	1%	-14%	22%
	$PM_{2.5}$	Proxy-based	123.8	113.3	34%	9%	0%	21%
		Unit-based	105.8		32%	-7%	-10%	23%

Table 2 The statistics for model performance of 1-hour-peak ozone and daily maximum 8-h averaged (MDA8) ozone concentration in July of 2014 with proxy-based and unit-based inventories

Species	Emission	SIM $\mu g/m^3$	OBS $\mu g/m^3$	NME	NMB	MFB	MFE
1h-peak ozone	Proxy-based	133.7	171.2	28%	-22%	-22%	32%
	Unit-based	135.0		27%	-21%	-21%	31%
MDA8 ozone	Proxy-based	115.1	128.1	23%	-10%	-9%	25%
	Unit-based	117.1		22%	-9%	-7%	24%

Table 3. The mean concentrations (unit: $\mu g/m^3$) of the components of $PM_{2.5}$ with proxy-based and unit-based inventories and their differences

Month	Emission	EC	OC	NO_3^-	SO_4^{2-}	NH_4^+
Jan	Proxy-based	41.2	49.7	11.8	11.7	7.8
	Unit-based	38.5	48.0	13.0	10.2	7.6
	difference	-7%	-4%	10%	-12%	-2%
Jul	Proxy-based	8.3	9.3	11.9	10.2	7.3
	Unit-based	7.1	8.4	11.8	9.3	6.9
	difference	-15%	-9%	0%	-9%	-5%